

# **Wear Rate Comparison of Different Impeller Materials for Pumping Various Types of Slurry**

by

**(Sandip Karmokar)**

A project submitted in partial fulfillment of the requirements for the degree of  
Master of Engineering in Mechanical Engineering



Khulna University of Engineering & Technology  
Khulna 9203, Bangladesh

May 2019

## Declaration

This is to certify that the project work entitled "*Wear Rate Comparison of Different Impeller Materials for Pumping Various Types of Slurry*" has been carried out by *Sandip Karmokar* in the Department of Mechanical Engineering, Khulna University of Engineering & Technology, Khulna, Bangladesh. The above project work or any part of this work has not been submitted anywhere for the award of any degree or diploma.

Signature of Supervisor



---

Dr. Sobahan Mia  
Professor

Department of Mechanical Engineering  
Khulna University of Engineering & Technology,  
Khulna, Bangladesh.

Signature of Candidate



---




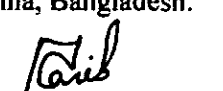
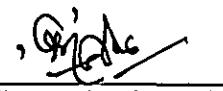
Sandip Karmokar  
Roll No: 1305555

Department of Mechanical Engineering  
Khulna University of Engineering &  
Technology, Khulna, Bangladesh.

## Approval

This is to certify that the project work submitted by *Sandip Karmokar* entitled "*Wear Rate Comparison of Different Impeller Materials for Pumping Various Types of Slurry*" has been approved by the board of examiners for the partial fulfillment of the requirements for the degree of *Master of Engineering in Mechanical Engineering* in the Department of *Mechanical Engineering*, *Khulna University of Engineering & Technology*, *Khulna, Bangladesh* in May 2019.

### BOARD OF EXAMINERS

1.   
Dr. Sobahan Mia  
Professor  
Department of Mechanical Engineering  
Khulna University of Engineering & Technology  
Khulna, Bangladesh. Chairman  
(Supervisor)
2.   
Head of the Department  
Department of Mechanical Engineering  
Khulna University of Engineering & Technology  
Khulna, Bangladesh. Member
3.   
Dr. Md. Shahidul Islam  
Professor  
Department of Mechanical Engineering  
Khulna University of Engineering & Technology  
Khulna, Bangladesh. Member
4.   
Dr. Md. Abdul Hasib  
Assistant Professor  
Department of Mechanical Engineering  
Khulna University of Engineering & Technology  
Khulna, Bangladesh. Member
5.   
Dr. Tarapada Bhowmick  
Professor & Vice-Chancellor  
North Western University  
Khulna-9100 Member  
(External)

## ACKNOWLEDGEMENT

With prodigious respect & delight, I would like to express my sincere thanks to **Professor, Dr. Sobahan Mia** for his cherished supervision & inspiration at each step of my project work. Most of the novel ideas and solutions in this project are the result of our plentiful inspiring discussion. This work would not have been possible without important guidance and inspiring of my supervisor **Dr. Sobahan Mia, Professor**, Department of Mechanical Engineering, Khulna University of Engineering & Technology.

It is my proud privilege to express regards and heartfelt thanks to **Dr. Md. Shahidul Islam, Professor**, Department of Mechanical Engineering, Khulna University of Engineering & Technology, for his guide and giving moral support to the project work.

I wish to express my gratefulness to **Dr. Md. Abdul Hasib, Assistant Professor**, Department of Mechanical Engineering, Khulna University of Engineering & Technology, for his guidance and encouragement for my project work.

I would like to thank all the teachers of Mechanical Engineering Department of Khulna University of Engineering & Technology for their endless support.

I would like to thank all the officers and staffs of the Machine shop, Welding shop and Wood shop of Mechanical Engineering Department, Khulna University of Engineering & Technology for their everlasting support.

Date:  
Place: Khulna

Sandip Karmokar  
Department of Mechanical Engineering  
Roll No: 1305555

## ABSTRACT

Erosive wear can be defined as a solid deduction process from a solid superficial due to frictional action between the slurry and surface. It is triggered by the effect of solid particles contained by slurry in contradiction of the surface of a solid body. The impacting solid particles progressively take away material from the solid superficial due to cutting action. Erosive wear is a significant factor for design centrifugal pump impeller and pumping slurry. Impeller wear is a very common phenomenon for every industry and slurry transportation system. Slurry erosion takes place in our civilized life such as thermal power plants, hydro power plants, excavating businesses, food handling productions, construction and civil works, oil field, solid-liquid hydro transportation systems, coal liquefaction plants, and boilers.

As the slurry erosion related machinery or equipment demand is becoming so acute day-by-day, scientists are giving efforts on the aptitudes of utilizing applicable technologies to reduce erosion from the related machinery or equipment. As a result performance of slurry equipment, dependability and operation lifetime of the slurry equipment are significantly improved.

Slurry erosion tester ordinarily used to investigate the comparative erosion behavior and characteristics of various materials exposed to slurry at moderate solid concentrations. Slurry erosion tester is a modest and convenient apparatus to determine slurry erosion of different equipment.

In this project, a pin mill type slurry-pot wear tester has been made. Total four types (aluminum, brass, mild steel and cast iron) of material with two geometries (flat bar and impeller) have been made for test. Slurry has been made by mixing silica sand and water by at required ratio in a GI container (slurry pot). All samples have been tested by the developed apparatus and determined wear rate with respect to various parameters like slurry density, shaft speed, impact angle and time. This apparatus is used for performing experiments on numerous samples of dissimilar materials exposed to slurry erosion.

In this experiment, total four types of impeller material with two geometries is used for testing at different operating condition such as impact angle, velocity, density and time. Among the eight samples brass is more erosive for both type of geometries (Flat bar and Impeller). On the other hand, cast iron is less erosive for impeller type geometry (45-degree impact angle) but for flat bar type geometry (0-degree impact angle) mild steel is less erosive. If impact angle and density are increased, erosion is found to increase for all types of materials and geometries. From the obtained results, it is clear that by this testing apparatus different types of materials can be tested and suitable pump impeller materials for different application can be found out.

1	Chapter I Introduction .....	1
1.1	General.....	1
1.2	Wear .....	2
1.3	Types of Wear: .....	2
1.4	Types of Erosive Wear .....	3
1.5	Objectives.....	5
2	Chapter II: Literature review .....	6
2.1	Background of Study .....	6
3	CHAPTER III: Pumps and Impeller.....	12
3.1	Pump.....	12
3.2	Centrifugal Pump.....	12
3.3	Working Principle .....	13
3.4	Main Components of Centrifugal Pump.....	14
3.5	Materials of Centrifugal Pump .....	16
4	CHAPTER IV: Design and Fabrication .....	17
4.1	Design of Slurry Erosion Pot Tester.....	17
4.2	Design Calculation.....	17
4.3	Fabrication of Slurry Erosion Tester .....	23
4.3.1	Fabrication of Main Structure .....	23
4.3.2	Fabrication of Shaft .....	24
4.3.3	Fabrication of Slurry Pot.....	24
4.3.4	Fabrication of Pulley.....	25
4.3.5	Motor .....	26
4.3.6	Fabrication of Control Box. ....	26
4.3.7	Fabrication of Samples .....	27
4.4	Slurry Erosion Tester Fabrication.....	30
4.5	Working Principle .....	31
4.6	Experimental Parameters: .....	31
4.7	Experimental Data of Erosion Measurement.....	32

5	Chapter V: Results and Discussion .....	38
<b>5.1</b>	<b>Erosion Measurement .....</b>	<b>38</b>
5.1.1	Erosion of Aluminum Sample .....	39
5.1.2	Erosion of Brass Sample.....	41
5.1.3	Erosion of Cast Iron.....	44
5.1.4	Erosion of Mild Steel.....	47
<b>5.2</b>	<b>Comparison.....</b>	<b>50</b>
6	Chapter VI: Conclusion .....	54
	FUTURE SCOPE.....	55
	REFERENCES .....	56

### List Figure

Figure 2.1:	Schematic diagram of slurry erosion pot. ....	7
Figure 2.2:	Schematic diagram of slurry erosion jet tester.....	8
Figure 2.3:	Schematic diagram of Coriolis erosion tester. ....	9
Figure 2.4:	Schematic diagram of whirling arm tester. ....	9
Figure 3.1:	Types of pump .....	13
Figure 3.2:	Centrifugal pump working principle.....	14
Figure 3.3:	Main components of centrifugal pump. ....	14
Figure 3.4:	Different types of impeller.....	15
Figure 3.5:	Centrifugal pump casing .....	15
Figure 4.1:	Correlation between power number and Reynolds number for Rushton turbine, paddle and marine propeller without sparing [21]. ....	20
Figure 4.2:	Main structure of slurry erosion tester. ....	23
Figure 4.3:	Shaft of the slurry erosion tester. ....	24
Figure 4.4:	Erosion tester slurry pot with lid.....	24
Figure 4.5:	Different diameter pulley for shaft. ....	25
Figure 4.6:	Motor pulley of the erosion tester.....	25
Figure 4.7:	Control box of the slurry erosion tester. ....	26
Figure 4.8:	Flat bar type sample.....	27
Figure 4.9:	Impeller type sample.....	27
Figure 4.10:	Flat bar type aluminum sample.....	28
Figure 4.11:	Impeller type aluminum sample. ....	28

Figure 4.12: Flat bar type brass sample.....	28
Figure 4.13: Impeller type brass sample. ....	29
Figure 4.14: Flat bar type mild steel sample. ....	29
Figure 4.15: Impeller type mild steel sample. ....	29
Figure 4.16: Flat bar type cast iron sample. ....	29
Figure 4.17: Impeller type cast iron sample. ....	30
Figure 4.18: Slurry pot tester with different main components. ....	30
Figure 5.1: Erosion of aluminum sample. ....	39
Figure 5.2: Microscopic view of aluminum sample erosion. ....	40
Figure 5.3: Erosion characterizes of Al sample at different speed, impact angle and time. ....	40
Figure 5.4: Erosion characteristic of Al sample at different speed, density, impact angle and time. ....	41
Figure 5.5: Erosion of brass sample. ....	42
Figure 5.6: Erosion characterizes of Br sample at different speed, impact angle and time. ....	43
Figure 5.7: Erosion characterizes of Br sample at different speed and impact angle.....	43
Figure 5.8: Erosion characterizes of Br sample at different speed, density, impact angle and time. ....	44
Figure 5.9: Erosion of Cast irons ample.....	45
Figure 5.10: Erosion of CI sample with respect to time at different speed, impact angle, constant density. ....	46
Figure 5.11: Erosion characterizes of CI sample at different speed, impact angle and constant density.....	46
Figure 5.12: Erosion characterizes of CI sample at different speed, density, impact angle and time. ....	47
Figure 5.13: Erosion of mild steel sample.....	48
Figure 5.14: Erosion characterizes of MS sample at different speed, impact angle and constant density. ....	49
Figure 5.15: Erosion of MS sample at different speed, impact angle, constant density and time.....	49
Figure 5.16: Erosion of MS sample with respect to slurry density at different speed and impact angle. ....	50
Figure 5.17: Erosion varies with shaft speed at 0-degree impact angle and constant density.....	51
Figure 5.18: Erosion varies with shaft speed at 45-degree impact angle and constant density.....	51
Figure 5.19: Erosion varies with slurry density at 0-degree impact angle and constant speed. ....	52
Figure 5.20: Erosion varies with slurry density at 45-degree impact angle and constant speed. ....	52



## LIST OF TABLE

---

Table 4.1: Design parameter of slurry erosion pot tester .....	21
Table 4.2: Shaft speed calculation of the erosion tester .....	22
Table 4.3: slurry properties. ....	31
Table 4.4: Aluminum sample erosion at 45-degree impact angle, different speed and constant density.....	32
Table 4.5: Aluminum sample erosion at 45-degree impact angle, different speed and various density .....	32
Table 4.6: Aluminum sample erosion at 0-degree impact angle, different speed and constant density.....	32
Table 4.7: Aluminum sample erosion at 0-degree impact angle, different speed and various density. ....	33
Table 4.8: Brass sample erosion at 45-degree impact angle, different speed and constant density. ....	33
Table 4.9: Brass sample erosion at 45-degree impact angle, different speed and various density.....	33
Table 4.10: Brass sample erosion at 0-degree impact angle, different speed and constant density. ....	34
Table 4.11: Brass sample erosion at 0-degree impact angle, different speed and various density.....	34
Table 4.12: Mild Steel sample erosion at 45-degree impact angle, different speed and constant density. ....	34
Table 4.13: Mild Steel sample erosion at 45-degree impact angle, different speed and various density.....	35
Table 4.14: Mild Steel sample erosion at 0-degree impact angle, different speed and constant density. ....	35
Table 4.15: Mild Steel sample erosion at 0-degree impact angle, different speed and various density.....	35
Table 4.16: Cast Iron sample erosion at 45-degree impact angle, different speed and constant density. ....	36
Table 4.17: Cast Iron sample erosion at 45-degree impact angle, different speed and various density.....	36
Table 4.18: Cast Iron sample erosion at 0-degree impact angle, different speed and constant density .....	36
Table 4.19: Cast Iron sample erosion at 0-degree impact angle, different speed and various density.....	37
Table 5.1: Impeller type different samples erosion at constant density. ....	38
Table 5.2: Flat bar type different samples erosion at constant density. ....	38
Table 5.3: Impeller type different samples erosion at constant speed.....	38
Table 5.4: Flat bar type different samples erosion at constant speed.....	39

## Nomenclature

$\rho_m$	Density of slurry (kg/m <sup>3</sup> )
$c_w$	Concentration of solids by weight in the slurry (%)
$\rho_s$	Density of the solids (kg/m <sup>3</sup> )
$\rho_l$	Density of liquid without solids (kg/m <sup>3</sup> )
$w_s$	Weight of dry solids
$w_l$	Weight of liquid phase
$c_v$	Concentration of solids by volume, %
$\Phi$	Volume fraction
$\mu_m$	Viscosity of slurry mixture, Pa. s
$\mu_L$	Viscosity of liquid in slurry mixture, Pa. s
$\mu$	Viscosity of slurry
$(Re)_i$	Reynolds number
$N_i$	Rotational speed(s-1)
$D_i$	Impeller diameter
$P$	Power
$N_p$	Power number
$N_s$	Shaft speed (rpm)
$N_m$	Motor speed (rpm)
$D_m$	Driver pulley diameter (inch)
$D_s$	Driven pulley diameter (inch)

# CHAPTER I

## Introduction

### 1.1 General

Slurry erosion, can be comprehensively defined as the procedure whereby the material is lost from a surface in contact with a moving molecule laden fluid by mechanical contact [1]. Wear occurs mainly due to erosion and the mechanism of erosion is greatly dependent on the processes parameters involved. The constraint that affect the erosion wear in case of pumping different type of slurry are pump impeller materials quality, materials of target surface, slurry concentration, impact velocity, impact angle, size and shape of solid particle containing in the slurry, slurry viscosity, and environment. However, due to difficulty to find out common causes and remedy of erosion. researcher all over the world have been trying to reduce the slurry erosion by taking various techniques such as uses right materials, impact angle, target materials surface coating ,optimizing pumping velocity [2].

Now a days, it is a massively egregious problem for the mechanical equipment's performance, reliability and operation life time in which solid liquid mixture is transported through pumps and pipes, used in many industrial applications like thermal power plants, hydro power plants, excavating activities, food handing out productions, manufacture and civil works, solid-liquid hydro shipping systems, oil field mechanical equipment, industrial boilers and coal liquefaction plants where coal is carried directly as a fuel in water or oil [3].

In Bangladesh, different types of pump and piping are used in many industrial applications like thermal and hydro power plant, construction works, Gas Field, Water treatment plant, Sewage water system, Sugar Industry etc. This large number of pumps and piping materials erode frequently due to wrong choice of materials. The consequences are the loss of material, loss of equipment reliability, increasing operational cost [4]. Therefore, use of right material for specific industrial application can save large number of money.

In this study, a pin mill type slurry-pot wear tester has been developed and different types of impeller material with various types of slurry has been tested to evaluate the erosion wear rate of different impeller material to decide suitable pump impeller material for pumping different slurry.

## **1.2 Wear**

Wear is the continuing elimination of material obtained at contacting surfaces due to relative motion between that surfaces or surfaces and fluid. Friction is the causes of energy loses and reduce the lifetime of the mechanical machinery and equipment. On the other hand, wear related with increased overhauling cost, preservation costs and costly machine downtime. Wear phenomena are closely related to frictional processes. Wear phenomena are profoundly influenced by the circumstance that most engineering surfaces are rough due to roughness of the surface frictional force are created and due to this frictional force wear is occurred.

## **1.3 Types of Wear:**

### **1. Erosive Wear:**

Erosive wear can be defined as the material removal process from a solid surface due to frictional force between the surface and the impact solid particle contains in liquid that is flowed through the solid surface [5]. Erosive wear is executed within a short time interval and it depends on the solid particle impact angle on solid surface, which may be vary from 0 to 90 degree and wear depends on among the fluid particle interaction, fluid particle and liquid particle interaction and particle – particle interaction [6].

The degree of erosive wear is reliant upon a number of aspects. The material individualities of the particles, such as their shape and grain structure, hardness of materials, slurry velocity and impingement angle are primary factors along with the properties of the surface being wrinkled. Erosive wear is occurred in pump impeller, pipes, volute casing, pipe fitting and turbine. Erosion wear must be considered in the design and operation in case of handling slurry.

### **2. Abrasive Wear:**

Abrasive wear occurs when either a hard particles or hard surface pass through a comparatively soft surface and finally causing loss of material from the soft surface.

The abrasive furrows can be found on the wear paths of the sliding friction between analogous metals. It means that abrasive particles may be made during the wear process due to work toughening, phase conversions and third body construction at the interface. Abrasive wear occur when hard asperities or third phase particles wipe under load compared to a comparatively softer surface. If the wear progression encompasses only two materials, it is known as two-body abrasive wear. If superfluous abrasive particles are used one has three-body wear. In general, wear rates for two-body wear are higher than for three body.

### **3. Adhesive Wear**

Adhesive wear takes place while two metals rub together with sufficient pressure to removal of metal from the less wear resistant metal surface. This wear is dependent on physical and chemical properties such as presence of corrosive atmosphere or chemicals, solid properties, as well as the dynamics such as the rapidity and applied load.

There are many reasons of adhesive wear and galling, all of which can be prevented through the proper design, manufacture and use of the machinery components.

### **4. Fatigue Wear**

Fatigue wear is a type of wear where a number of cycles is required to generate debris. The fatigue procedure in metals may prompt the generation of surface and subsurface cracks, which after a critical number of cycles results in a severe damage, such as large fragments leaving the surface. There are two mechanisms of fatigue wear, which are high- and low-cycle fatigue. In high-cycle fatigue, the number of cycles before failure is high, so the component life is relatively long. In the low-cycle fatigue, the number of cycles before failure is low, so the component life is relatively short.

### **5. Corrosive Wear**

Corrosive wear may be defined as the wear when any components works in a corrosive media (liquid, gas or solid). The main reason of this wear is tribochemical reaction between corrosive agent and the bulk material generates a reaction (protective) layer on the surface. During the sliding friction, this layer is removed and the tribochemical reaction is started again. If the growth of the layer is faster than its removal, then only this layer is worn and not the bulk material directly. However, if the growth and removal of the layer is too fast, then there is an excessive wear of a bulk material through the reaction film.

## **1.4 Types of Erosive Wear**

### **1. Solid Particle Impingement**

Solid particle impingement erosion can be defined as such kind of erosion created by a continuing series of impacts from solid particles on a solid surface. When solid particle contain in slurry, impact on solid surface due to friction metals are wear from the surface. Solid particle impingement erosion depends on the following criteria.

Solid particles velocity, impingement angle, particle size, strength of particles, temperature, ductility of surface, particles hardness. Solid particle impingement erosion occurs in sandblast equipment, water jet cutting, abrasive cutting, coal plants (transport of pulverized coal), gas turbines, power plants pipelines.

## **2. Liquid Droplets Impingement**

Liquid droplets impingement erosion can be defined as such kind of erosion created by a ongoing series of impacts from a jet of fluid on a solid surface. When solid particle contain in slurry, impact on solid surface due to friction metals are wear from the surface. Liquid droplets impingement erosion happens in elbow pipe, aircraft rainfall during flying condition.

## **3. Cavitation**

Cavitation-corrosion is continuous removal of material from an equipment solid surface due to erosion caused by the "implosion" of gas bubbles on a metal surface. It frequently related with rapid differences in pressure related to the hydrodynamic parameters of the fluid (e.g. hydraulic turbine blades, propellers, stirrer blades, etc.). A regular hydraulic governance, in the fluid is tremendously important.

A good smooth surface situation decreases the chance of vapor bubbles formation. Vapor bubbles formation depends on pressure. If pressure increase then chance of vapor bubbles formation decrease and by this way maintain single phase fluid. Plastic or rubber coatings have often proved to be effective, although the problems of adherence between the coating and the metal are frequently an obstacle. It occurs in Pumps, mixing impellers, ultrasonic device.

## **4. Slurry Erosion**

Slurry erosion can be defined as the progressive loss of material from an equipment solid surface by the action of a mixture of solid particles in a liquid (slurry) in motion with respect to the solid surface [7]. It occurs in drilling operation in oil, liquid or slurry pumping and mineral beneficiation. The rate of erosion wear depends on various parameter such as Slurry concentration, Speed of rotation, Distance traversed and Time. Slurry erosion can be determined by varying different experimental conditions and taking different materials sample and also surface treated samples.

Slurry erosion is the procedure whereby the material lost from a mechanical tools surface in contact with a moving molecule loaded fluid by mechanical interaction. It is a very difficult issue for the performance, reliability, operation life of the slurry handling equipment in which strong fluid blend moved through pumps and pipes.

Areas Where Slurry Erosion Takes Place are Given Below

- a) Thermal power plants, Hydropower plants, Industrial boilers
- b) Oil drilling, Pumping, Mining industries
- c) Agriculture equipment, Food processing industries
- d) Construction and Civil works
- e) Solid-liquid hydro transportation systems, Coal liquefaction plants
- f) During milling and transportation of ores through pipes and pumps
- g) Abrasive jet cutting

Factors Affecting Erosion Wear are Given Below

- a) Attack angle
- b) Velocity of impact particle
- c) Hardness of metal
- d) Particle size and shape
- e) Concentration of Slurry
- f) Distance of fall
- g) Force of impingement

Erosion Rate

Erosion rate is the rate of material loss (erosion) from a solid surface with respect to time. Erosion rate may be defined by the following formula.

$$\text{Erosion rate} = \frac{\text{Loss of materials}}{\text{Time}}$$

## 1.5 Objectives

The specific objectives of this project are

1. To design and fabrication of a pot type slurry wear tester.
2. To test sample materials (Cast Iron, Aluminum alloy, Brass) for various types of slurry concentration and particle size.
3. To measure wear rate at various shaft speed.
4. To determine the suitable pump impeller material for pumping different slurry.

## CHAPTER II

### Literature Review

#### 2.1 Background of Study

Laboratory experiments on slurry erosion are performed to comprehend the fundamental components of the wear procedure to investigate the impact on the performance, reliability, and operation life of the slurry apparatus used in many engineering applications.

Slurry erosion testing method can be divided in to two categories one is tube wear tests and another is laboratory simulation tests [8]. Simulation testing is broadly embraced due to low expense, moderately simple to set up and work, and fast to deliver results. On the other-hand pipe wear test is used for industrial application for testing of pipes, pipe samples. Wear caused by the mechanical interaction between slurry flow and pipe flow is recorded by weighing. Though some study was carried out by tube wear testing. The major drawbacks pipe wear testing are high cost, and required long times.

A varied range of apparatuses has been designed to compartment laboratory-scale slurry erosion studies but among of them two test arrangements such as slurry pot tests and slurry jet tests are more popular.

Slurry pot tester is used for the investigation work on slurry erosion, as illustrated elsewhere [9-12] and graphic diagram of such kind of test device is shown in figure 2.1. This category of a slurry device has guileless design and it is easy to construction. Tsai et al introduced a slurry pot and similar one was designed and fabricated by Gupta et al. in 1995. Such pot testers are easy to operate and provide rapid results for ranking resistance to slurry erosion of different materials. They have been successfully used to characterize erosion resistance and to provide data for selection of materials. The pot tester results were reported to agree reasonably well with pipeline wear. Pot tester has advantages and as well as disadvantages. However, because of the unstable inertia flow of the slurry, it is very difficult to measure and control the velocity and impingement angle of the slurry accurately. In addition, the test is further complicated by blunting and crushing of the impacting particles during the test.

Pot tester has advantages and as well as disadvantages. The disadvantages of ths testing apparatus are the difficulty in controlling the flow conditions, real density of impacting particles, slurry temperature, impinging angle and velocity. In contrast to jet type, this test device is easier to use, manufacture and very cheap. A major favorable position of this test device is the capacity to quickly conduct four samples of various materials in contrast with other test rigs with this equivalent disintegration power.



Jet tester was designed some years ago and used for the research work on slurry erosion, as illustrated elsewhere [13-16]. According to name of this type apparatus, slurry (liquid with solid elements) as a jet impact the goal material which may be standing or revolve. In rigs with rotating specimens, a specimen crosses a slurry jet, causing cyclic collisions. In case of devices with a stationary specimen, a specimen continuously is exposed to a slurry jet. Jet tester has advantages and as well as disadvantages. The impingement point of every solid molecule does not continue as before during the test and it is difficult to get a high effect speed because of the high viscosity of the slurry. Furthermore, the impact velocity must be estimated and aligned intermittently in light of the wear of the nozzle. Moreover, as the slurry stream is locally focused on the sample surface, it does not simulate well the slurry erosion phenomenon as it occurs in the practical field. In this way, assessment of erosive wear by mass loss can't give data on the nearby seriousness and dissemination of wear. A schematic diagram of a jet impingement tester is shown in figure 2.2.

In this mechanical assembly, specimen are mounted into the end of four arms, which are connected to a rotor and affected by a falling slurry stream. This test is performed in a vacuum to avoiding aerodynamic consequences for the slurry stream. This test rig can measure erosion velocity and impingement angle precisely and apparatus control is very easy.

In addition, fresh slurry continuously impacts the specimens. The whirling-arm tester simulates a fan operating in a slurry spray, and to some extent, the erosion of a pelton turbine. It used for studies on erosion wear resistance of blades of helicopter rotors and gas turbine compressor.

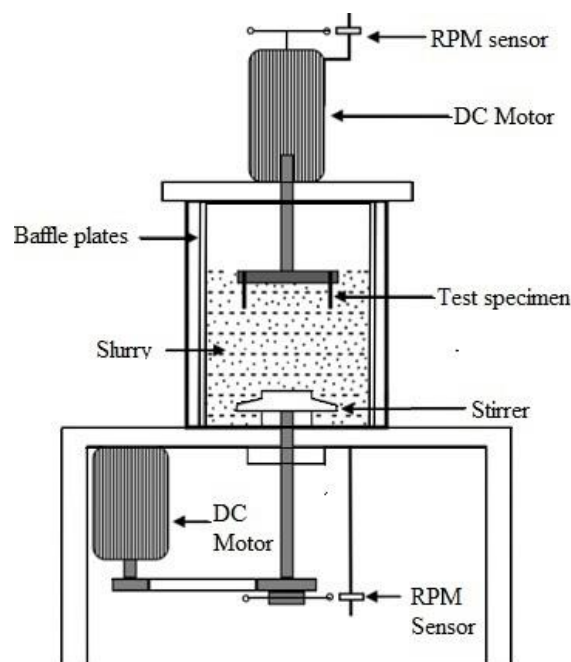


Figure 2.1: Schematic diagram of slurry erosion pot.

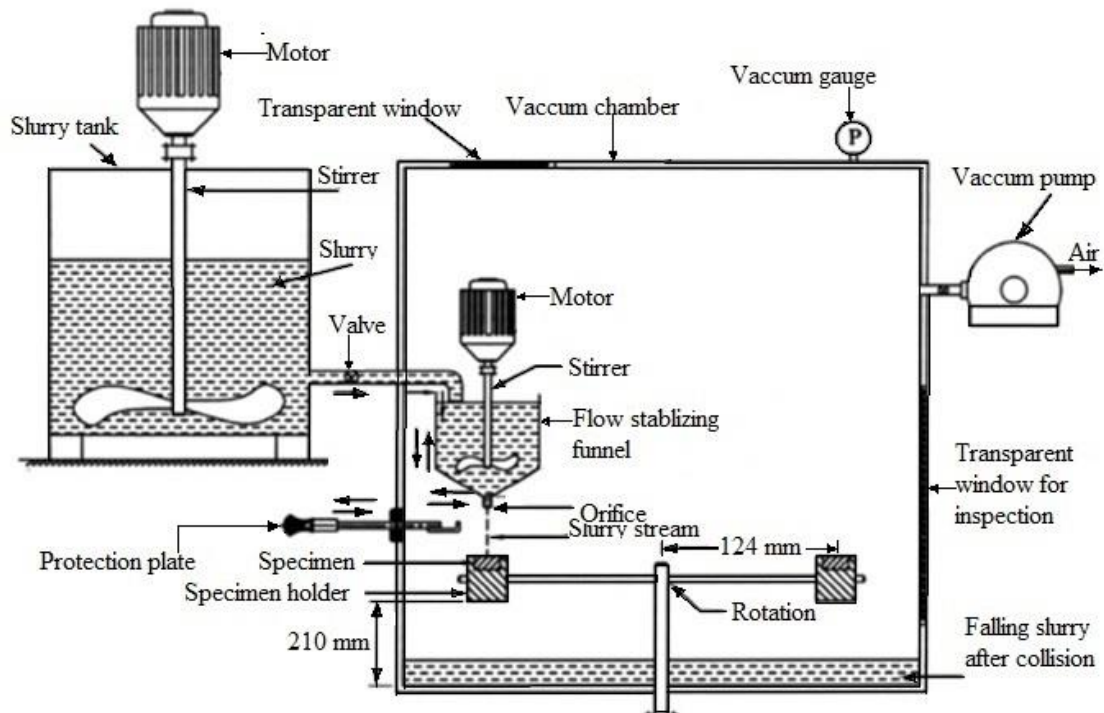


Figure 2.2: Schematic diagram of slurry erosion jet tester.

Coriolis erosion tester was firstly fabricated and introduced by Tuzson in 1984 [16], to investigate the movement of slurries and their interaction with surfaces such as pumps and pipelines. Tuzson developed Slurry erosion tester was modified by Clark et al. in 1999 to adapt the device for using flat test specimens with dimensions of 29 x 15 x 6 mm [17]. Schematic diagram of Coriolis erosion tester is shown in Figure 2.3. Coriolis slurry tester utilizes centrifugal and Coriolis powers. Freshly arranged slurry from holder bolstered into the focal point of the rotor (distance across 150 mm), where is a slurry channel port (measurement 12.7 mm). The sample holders are situated at equivalent good ways from the focal point of revolution of the rotor.

In the sample, holders are the channels through which flows the slurry, while the base of the channel forms the test specimen. The channels are 1 mm wide and 6.35 mm high with rectangular cross-section. The test example pivots at an accelerate to 7000 rpm. The analyzer utilizes an electric engine of 1.5 kW and speed controller under low effect edge. Slurry is quickened outwards by divergent power, while affected by Coriolis power erodent particles choose the outside of the test sample, accordingly expanding the collaboration of the slurry with the outside of the sample. Because of high turn speed, this strategy abbreviates the testing time. The structure of the tester permits testing at the same time two samples [18].

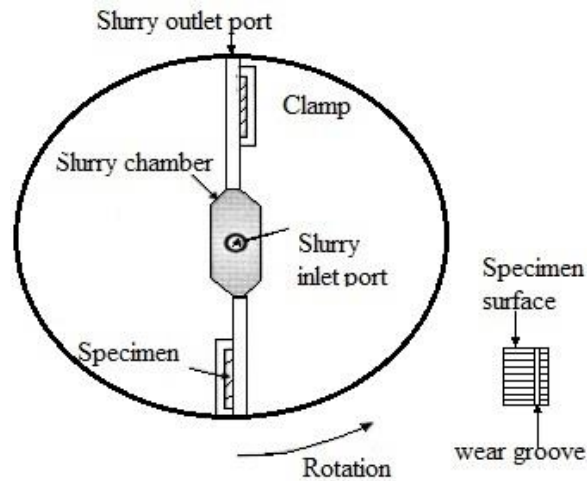


Figure 2.3: Schematic diagram of Coriolis erosion tester.

The whirling arm test device was developed by Lin and Shao is shown in below Figure 2.4 [19]. The slurry tank (25 L in limit) contains a blend of strong particles and water, which are mixed utilizing a stirrer. Then, prepared mixture streams to the following tank in the shape of a funnel with a stirrer. It is essential that the mixture is variegated appropriately. The test device has four horizontal arms, on which placed test specimens. The arms are joined to a shaft. During the test, on test specimens falling jet from the slurry tank (funnel-shaped) with a velocity of 1.62 m/s. An important feature is the capability to fine alteration of impact angle ( $0^{\circ}$ - $90^{\circ}$ ) and impact velocity. Tests are carried out in a vacuum (up to 37.3 kPa) because the authors wanted to eliminate the effect of airflow (aerodynamic effect) on the slurry stream.

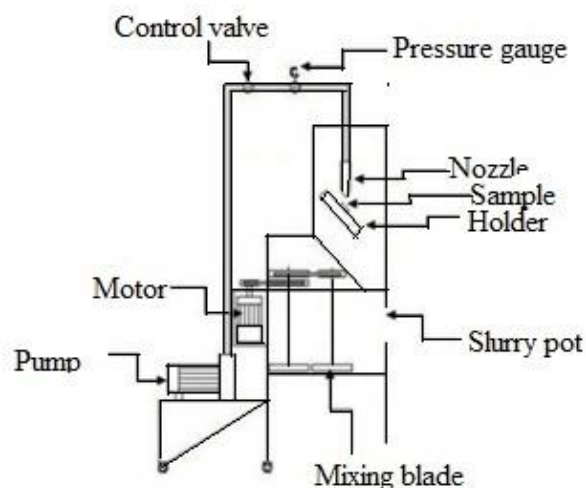


Figure 2.4: Schematic diagram of whirling arm tester.

In the present work, a pin mill type slurry-pot wear tester has been developed. Flat type and impeller type samples with two different geometries has been tested by the developed tester. By this testing apparatus different types of material can be tested at various speed and concentration. Total four types of material such as Aluminum, Brass, Mild Steel and Cast Iron has been tested by taking different types of slurries to find out the wear characteristics of the material by measuring the rate of mass loss with respect to various parameters like slurry concentration, speed of rotation, distance traversed, impact angle and time. The apparatus has been tested by taking slurry of silica sand in a GI compartment to discover the rate of mass loss of aluminum, brass, mild steel, cast iron test. This machine can be utilized for completing trials on different examples of various material, which are exposed to slurry disintegration. By this device slurry wear rate of various material can be estimated and can settle on choice which materials is reasonable for which application.

Slurry erosion seriously depends on attack angle, defined as the angle between the aim surface and the path of striking velocity of the slurry contained solid particle. The rate of mass reduction due to erosion is a role of impact angle of particles. The discrepancy of erosion wear with the impact angle is dissimilar for brittle and ductile materials. The extreme erosion happens at 20-30degrees impact angles for ductile materials. Whereas, the extreme erosion wear happens at 90-degree impact angle in case of brittle materials.

Slurry erosion also seriously depends velocity of solid particle and has significantly effects on erosion wear. The rate of materials removal has prevailing effect impact velocity. Due to increasing velocity of particle, there is significant proliferation in erosion rate. The erosion rate is related to the particle velocity using power law. Correlation in which the power index for velocity varies in the range of 2-4 Gandhi et al (1999), evaluated the erosion rate is a function of velocity [18].

$$\text{Erosion rate} = f(\text{velocity}^{2.6})$$

Hardness is the characteristic of a solid material articulating its resistance to enduring distortion. Materials superficial hardness as like solid particles hardness has profound effect on the erosion wear mechanism. The ratio of goal material hardness and solid particles hardness is called hardness ratio. Gandhi et al. (2008) developed a correlation between hardness ratio of particle to metal  $K_{(HP/HT)}$  and erosion rate.

Molecule size and shape is likewise one of the conspicuous parameter, which influence disintegration wear. Numerous specialists have considered strong molecule size imperative to disintegration. The disintegration wear increments with increment in molecule size as indicated by power law relationship.

The impact of molecule shape on the erosion is extremely troublesome because of challenges in characterizing the distinctive shape features. Generally, roundness factor is thought about. On the off chance that roundness factor is considered, If roundness factor is considered then the particles are perfectly spheres and lower values show the particle angularity [19].

Concentration is measure of strong particles by weight or by volume in the liquid. As attentiveness of particle increases more particles strike the superficial of impeller, which increment the disintegration rate, the centralization of slurries can change from 2% to half contingent on the kind of slurry. In any case, at extremely high focuses molecule collaboration increments and these abatements the striking speed of molecule superficially.

Slurry erosion depends on distance between slurry injection point and solid sample. If distance of fall is increase then the erosion rate will be decrease.

Slurry erosion depends on kinetic energy of impinging particle. If kinetic energy is high then frictional force between the solid particle and sample surface will be high. Due to high frictional force, erosion will increase significantly.

## **CHAPTER III:**

### **Pumps and Impeller**

#### **3.1 Pump**

A pump is a hydraulic machine that transforms mechanical energy into hydraulic energy (in form of pressure head) and transfers fluids (liquids, semi liquid, gases or sometimes slurries) from lower pressure to higher pressure by mechanical action. Pumps operate by some mechanism typically reciprocating or rotary. Pump also consume energy to perform mechanical work for transferring the fluid and the sources of energy are manual operation, electricity, tidal power, engines, wind power, solar power and hydraulic energy.

Pump can be classified mainly as two categories, one is positive displacement pump and another is rotodynamic pump as shown in figure 3.1. Positive displacement pump is a mechanical machine, which displaces the liquid from the suction side to the discharge side by mechanical variation of volume of chamber in the suction side to the discharge side.

A rotodynamic pump is a dynamic mechanism in which energy is uninterruptedly conveyed to the pumped liquid by means of a spinning impeller, propeller, or rotor, in contrast to a positive displacement pump in which a fluid is moved by trapping a fixed amount of fluid and forcing the trapped volume into the pump's discharge.

#### **3.2 Centrifugal Pump**

A centrifugal pump is a rotodynamic pump that converts mechanical energy into pressure energy. The method of energy exchange in fluids mechanism follows the Bernoulli principle. There are various types of centrifugal pumps such as single stage, multi stage, self-priming, non-priming, open impeller, semi closed impeller and enclosed impeller that is shown in figure 3.1.

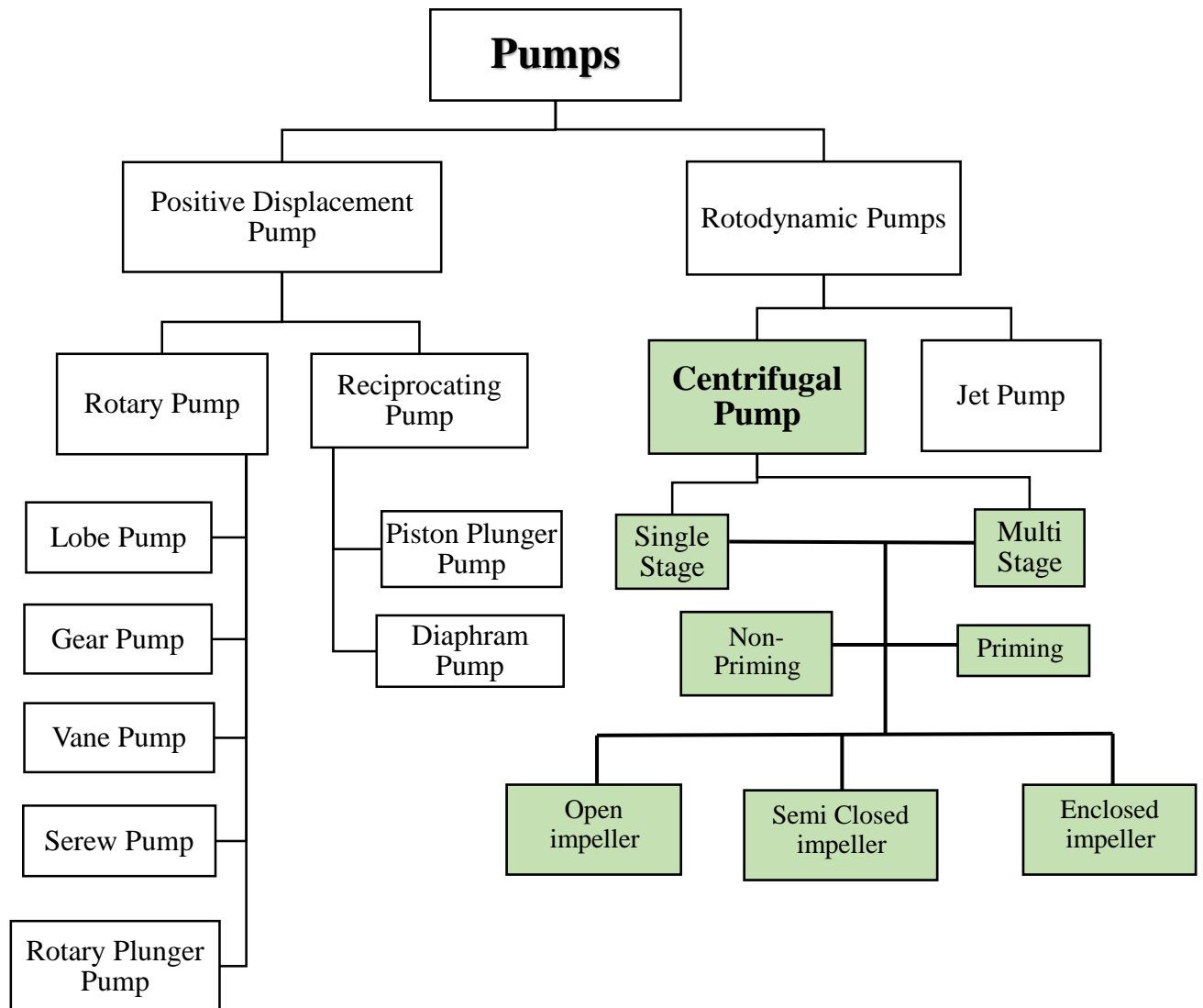


Figure 3.1: Types of pump

### 3.3 Working Principle

The fluid come in the pump close to the rotating axis, striking into the revolving impeller. The impeller includes a rotating disc with numerous attached vane, which are shown in below figure 3.2. The vanes generally slope backwards and away from the way of rotation. The fluid enters into the impeller and capture by impeller. The fluid is enhanced by pulse transmission while succeeding the curvature of the impeller vanes from the impeller center outwards. It reaches its maximum acceleration on the impeller and fluid has left the impeller, then it flows at a large area. Therefore, kinetic energy is converted to pressure energy as per Bernoulli's principle. When fluid is displaced from the delivery side of the pump, more fluid is sucked from suction side and thus fluid flow is created.

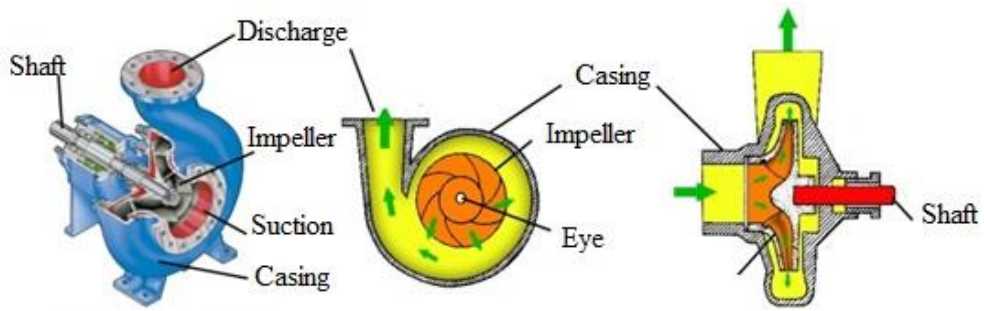


Figure 3.2: Centrifugal pump working principle.

### 3.4 Main Components of Centrifugal Pump

The main parts of centrifugal pump are Impeller, Casing, Suction pipe, Delivery Pipe and those are explained hereunder.

#### Suction Pipe

Suction pipe is coupled to the inlet of pump and other end dips into the water reservoir. Strainer and a one-way foot valve are fitted with suction pipe.

#### Delivery Pipe

A hollow pipe whose one end is coupled to the outlet of the pump and other end transports water to the prerequisite altitude or other device.

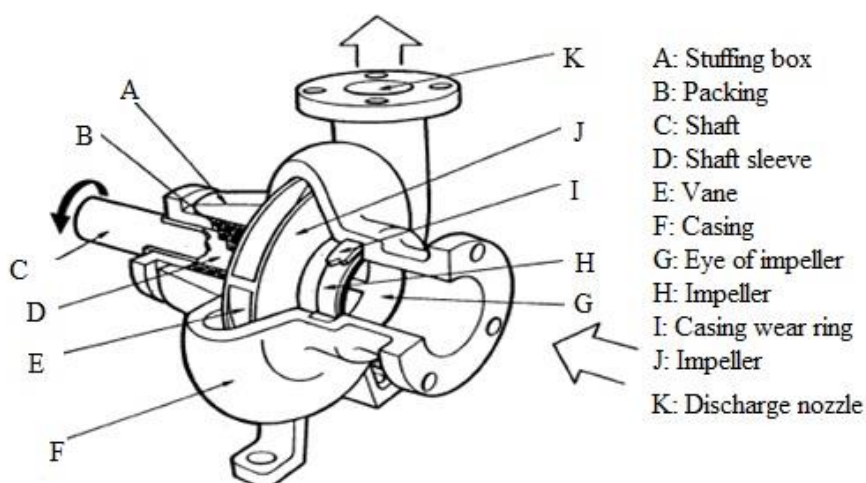


Figure 3.3: Main components of centrifugal pump.



## Impeller

The impeller is an essential part of centrifugal pump. It is made of by a sequence of backward curved vane that are shown in below figure 3.4. The impeller is connected with a rotating shaft. Generally, an impeller is made by iron, steel, aluminum, brass or plastic, while impeller for corrosive rough surface containing fluids and slurries require high-end materials for ensuring a pump long life [2]. The reliability and performance of the pump closely depends on the impeller diameters and design criteria. In general, there are three possible types of impellers, open, enclosed and semi open impellers those are shown in the following figure is suitable for a specific application.

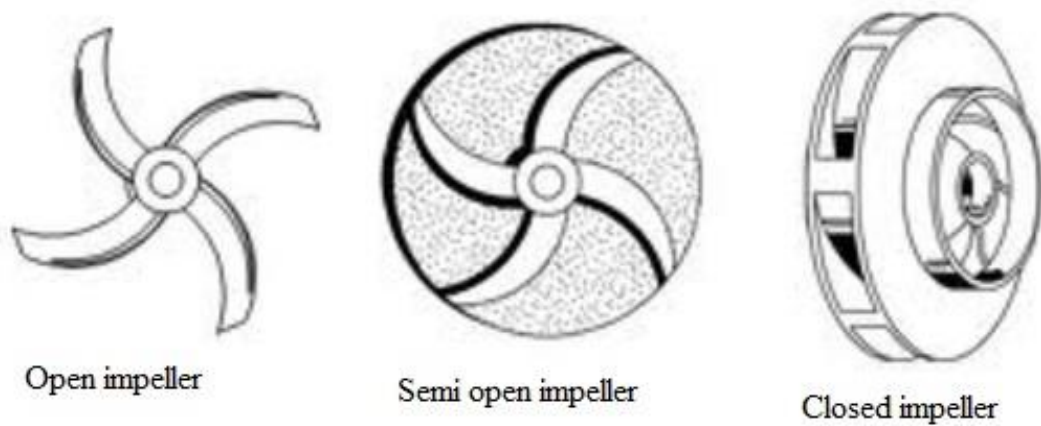


Figure 3.4: Different types of impeller.

## Casing

The pump's casing is a closed airtight passage surrounding the impeller and its main function is to convert kinetic energy of liquid into pressure energy. It supports the shaft bearings and takes the centrifugal forces of the revolving impeller and axial loads caused by pressure thrust disproportion. Different types of casing are shown below in figure 3.5. There are three types of casing.

- a. Volute Casing
- b. Vortex Casing
- c. Casing with guide blade

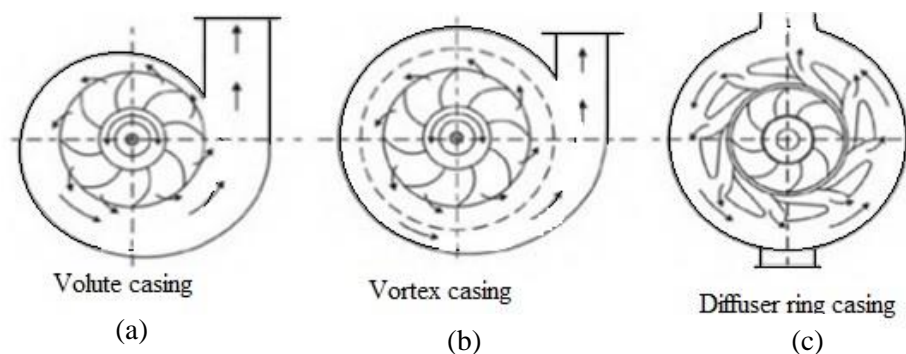


Figure 3.5: Centrifugal pump casing.

### 3.5 Materials of Centrifugal Pump

Pumps and pumps component materials are very important for pumps long life and performance. For this reason pumps and components are made up by different materials considering different criteria such as system requirements, pumping media type, and the surrounding environment condition. Some of the most common materials, which are used in pumps are discussed below:

**Cast iron:** Cast iron affords high tensile strength, toughness, and abrasion confrontation analogous to high-pressure ratings.

**Plastics:** Plastics are low-cost and provide wide-ranging confrontation to corrosion and chemical attack.

**Steel and stainless:** Steel and stainless steel alloys afford fortification in contradiction of chemical and rust corrosion and have higher tensile strengths corresponding to plastics, analogous to higher pressure ratings.

**Other materials:** Aluminum, Brass, Bronze, Ceramics, Nickel-alloy

When selecting the material type, there are a number of considerations that need to be taken into account as follows.

**Chemical compatibility:** Pump components in contact with the pumping slurry or product additives (cleaners, thinning solutions) should be made of chemically well-matched materials that will not consequence in extreme corrosion or adulteration.

**Explosion proof:** Non-sparking and explosion resistance materials are mandatory for working surroundings or media with particular predisposition to catching fire or explosion.

**Sanitation:** Pumps in the food, agriculture and beverage manufacturing necessitate high-density seals or seal less pumps that are relaxed to clean and disinfect.

**Wear:** Abrasives handling pumps necessitate virtuous wearing handling capabilities materials. Rigid and tough surfaces with chemically unaffected materials are often incompatible. The base and pump casing materials should be of satisfactory strength and also be able to hold up against the circumstances of its functioning situation.

## CHAPTER IV

### Design and Fabrication

#### 4.1 Design of Slurry Erosion Pot Tester

Slurry erosion pot tester is most popular because of its simple design and it is easy to manufacture. The main components of this tester are slurry pot, motor, shaft, frame and test sample. The operation of pot testers are very easy and afford quick results for standing resistance to slurry erosion of dissimilar materials. During design of this pot tester different variable such as speed, motor power, shaft diameter, main structure size, drain, lifting, speed reducer, belt size, slurry density, sample size, power source, etc. are take into consideration.

#### 4.2 Design Calculation

For design of the slurry pot tester consider maximum speed, maximum slurry density and paddle impeller due to maximum power required of paddle type impeller.

##### Average slurry density calculation:

Slurry is a mixture of a solid and a liquid. The density of a slurry can be calculated by the following equation (1).

$$\rho_m = 100 / [c_w / \rho_s + (100 - c_w) / \rho_l] \quad (1)$$

Where

$\rho_m$  = Density of slurry (kg/m<sup>3</sup>)

$c_w$  = Concentration of solids by weight in the slurry (%)

$\rho_s$  = Density of the solids (kg/m<sup>3</sup>)

$\rho_l$  = Density of liquid without solids (kg/m<sup>3</sup>)

Concentration of solids by weight in the slurry (%) can be calculated by the following equation (2).

$$c_w = \frac{W_s}{W_s + W_l} \quad (2)$$

Where

$w_s$ = Weight of dry solids

$w_l$ = Weight of liquid phase

For calculation maximum required power, consider maximum sand used in this project 9 kg and minimum water used in this project 6 kg. Concentration of solids by weight in the slurry (%) can be calculated from the equation (2).

$$c_w = \frac{9}{9+6} = 0.6 = 60\%$$

Now density of slurry can be calculated by equation (1) and considering sand density to be 1400 kg/m<sup>3</sup> and water density 1000 kg/m<sup>3</sup>.

$$\begin{aligned} \rho_m &= 100 / [60 / 1400 + (100 - 60) / 1000] \\ &= 1206.897 \text{ kg/m}^3 \end{aligned}$$

### Slurry Viscosity Calculation:

Volume fraction:  $\Phi = c_v / 100 \quad (3)$

Where:

$c_v$  = Concentration of solids by volume, %

$\Phi$  = Volume fraction

Solids concentration by weight ( $c_w$ ) solids concentration by volume ( $c_v$ ) are related to the solid density and the mixture density. Solids concentration by volume ( $c_v$ ) can be calculated by the following equation.

$$c_v = c_w * (\rho_m / \rho_s) \quad (4)$$

Where:

$c_v$  = Solid concentration by volume, %

The viscosity of a thinned slurry consisting of solids in a liquid can be calculated roughly from the volume fraction  $\Phi$  and the viscosity of the liquid using the following equation (5).

$$\mu_m = \mu_L * (1 + 2.5\Phi) \quad (5)$$

Where:

$\mu_m$  = Viscosity of slurry mixture, Pa. s

$\mu_L$  = Viscosity of liquid in slurry mixture, Pa. s

From equation (4)  $c_v = 60 * (1206.897 / 1000) = 72.41\%$

From equation (3)  $\Phi = 72.41 / 100 = 0.7241$

Now, considering the dynamic viscosity of water is  $8.90 \times 10^{-4}$  Pa. s at about 25 °C and from equation (5) viscosity of solid can be determined.

$$\mu_m = 8.90 \times 10^{-4} * (1 + 2.50 * 0.7241) = 4.04 \times 10^{-4} \text{ Pa. s}$$

### Reynolds number Calculation:

$$(Re)_i = (N_i D_i^2 \rho_m) / \mu \quad (6)$$

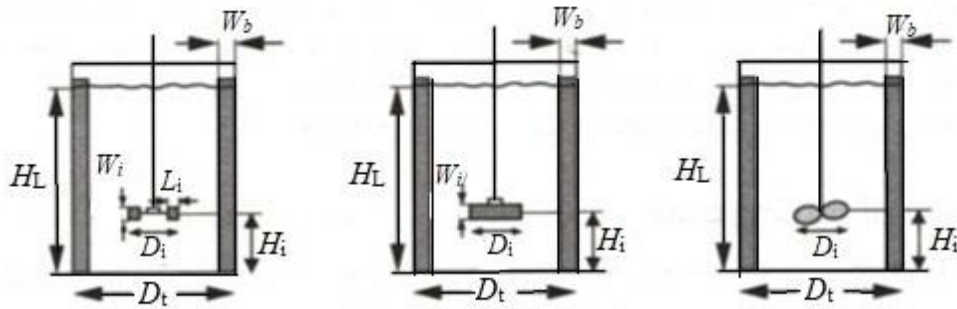
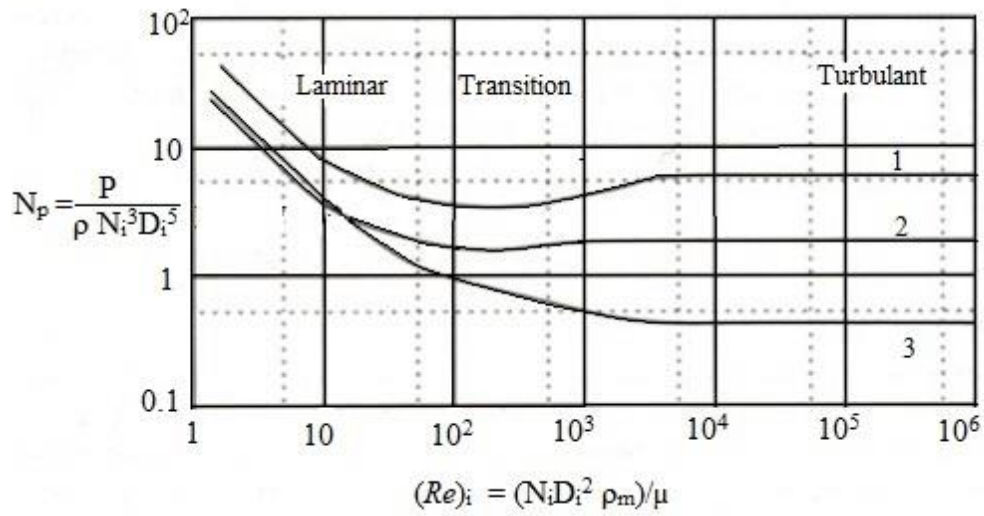
Where

$\mu$  = Viscosity of slurry

$(Re)_i$  = Reynolds number

$N_i$  = Rotational speed ( $s^{-1}$ )

$D_i^3$  = Impeller diameter



Impeller	$D_t/D_i$	$H_t/D_i$	$H_i/D_i$	Baffles	
				$W_b/D_t$	Number
1. Rushton turbine $W_i/D_i=0.2, L_i/D_i=0.25$	3	3	1	0.1	4
2. Paddle $W_i/D_i=0.25$	3	3	1	0.1	4
3. Marine propeller pitch= $D_i$	3	3	1	0.1	4

Figure 4.1: Correlation between power number and Reynolds number for Rushton turbine, paddle and marine propeller without sparing [21].

The relationship between dimensionless numbers impeller Reynolds number  $(Re)_i$  and the power number  $(N_p)$  of Newtonian fluids without gaseous form is shown in above figure 4.1.

**Motor power calculation:**

$$P = N_p \rho N_i^3 D_i^5 \quad (7)$$

Where

P = Power

$N_p$  = Power number

$N_i$  = Rotational speed( $s^{-1}$ )

$D_i^3$  = Impeller diameter

Diameter of the paddle type impeller 190 mm and maximum rotational speed  $N_i = 530$  rpm or  $8.83 s^{-1}$ . So Reynolds number can be calculated from the equation (6).

$$\begin{aligned} (Re)_i &= (8.83 * 0.19^2 * 1206.897) / 4.04 \times 10^{-4} \\ &= 9.52 \times 10^5 \end{aligned}$$

From Figure 4.1 for turbulent flow and Reynolds number  $(Re)_i$   $9.52 \times 10^5$  power number ( $N_p$ ) is 3. So, now power required for this apparatus can be calculated from the equation (7).

$$P = 3 * 1206.897 * 8.83^3 * 0.19^5 = 617.22 \text{ W}$$

If consider safety factor 2 then required power:  $617.22 * 2 = 1234.44 \text{ W}$ .

Due to unavailability of 1234.44 W capacity motor in market 1492 W motor is selected.

Considering above design calculation design parameter of the slurry pot wear tester which was used in this project has given in below table 4.1 and schematic diagram of this kind of test device is shown in figure 4.2.

Table 4.1: Design parameter of slurry erosion pot tester

Serial no.	Components	Design parameter
	Main structure	2.5 feet x 2.5 feet x 3 feet
1.	Shaft	Diameter 35 mm and length 650 mm.
2.	Pulley	4 stage pulley with different diameter (4, 5, 6, 7 inch).
3.	Slurry pot	Diameter 280 mm and height 250 mm.
4.	Motor	2 HP, single phase, 1450 rpm, 220 V.
5.	Belt	V- Belt, size-B.
6.	Flat bar type Samples	190mm X 28mm X 12 mm.
7.	Impeller type samples	190mm X 30mm X 10 mm.

### Shaft speed calculation for variable diameter pulley:

Considering the following parameter

Motor power : 2 HP  
Motor speed : 1450 rpm  
Driver pulley diameter : 2.5 inch  
Driven pulley diameter : 4,5,6 and 7 inch

Shaft speed can be calculated by the following equation (8).

$$N_s/N_m = D_m/D_s$$
$$N_s = (N_m D_m)/D_s \quad (8)$$

Where

$N_s$  = Shaft speed (rpm)

$N_m$  = Motor speed (rpm)

$D_m$  = Driver pulley diameter (inch)

$D_s$  = Driven pulley diameter (inch)

Considering motor speed 1450 rpm, driver and driven pulley diameter 2.5 inch and 4 inch from equation (8) shaft speed will be 906.25 rpm. By the same procedure others corresponding speed was calculated and showing in below table 4.2.

Table 4.2: Shaft speed calculation of the erosion tester

Sl. No.	Motor speed(rpm)	Driver pulley diameter (inch)	Driven pulley diameter (inch)	Shaft speed (rpm)
1	1450	2.5	4	906.25
2			5	725
3			6	604.14
4			7	517



### 4.3 Fabrication of Slurry Erosion Tester

Main components of slurry erosion tester are given below.

- |                   |                 |
|-------------------|-----------------|
| a) Main structure | e) Motor        |
| b) Shaft          | f) Belt         |
| c) Pulley         | g) Control box. |
| d) Slurry pot     | h) Samples      |

#### 4.3.1 Fabrication of Main Structure

The main structure is shown in figure 4.2. The frame is made by 1.5 inch V type GI angle. The main structure dimension is 2.5 feet length, 2.5 feet wide and 3 feet height.

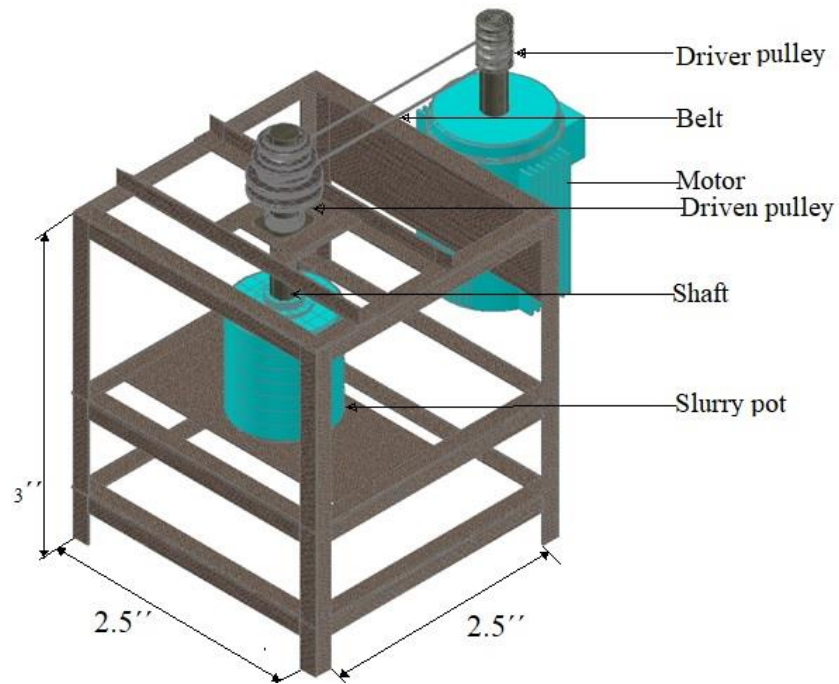


Figure 4.2: Main structure of slurry erosion tester.

### 4.3.2 Fabrication of Shaft

The shaft was made from a piece of 35 mm diameter mild steel rod having total length 650 mm. This shaft has two bearing holding grooves and one pulley holding grooves which was made by turning it in a lathe machine. This shaft is shown in the figure 4.3 given below.

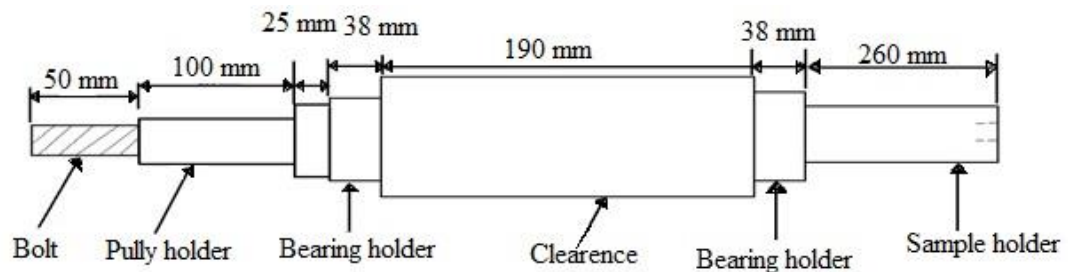


Figure 4.3: Shaft of the slurry erosion tester.

### 4.3.3 Fabrication of Slurry Pot

A slurry pot with lid has been made for this testing apparatus is shown in figure 4.4. The size of slurry pot is 28 mm diameter and 25 mm height. Slurry pot was made by 4 mm thickness GI plate. Main shaft is connected with slurry pot via pot lid by pillow type bearing housing.

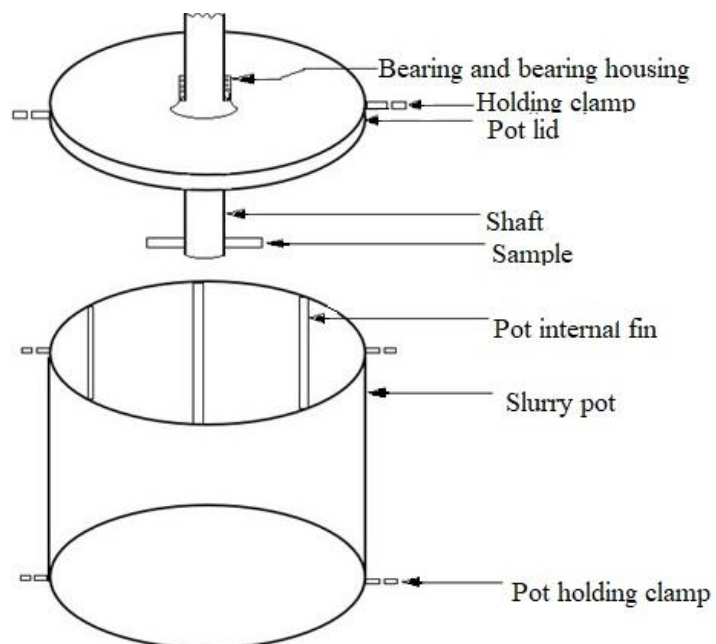


Figure 4.4: Erosion tester slurry pot with lid.

#### 4.3.4 Fabrication of Pulley

Pulley is a simple machine that increases mechanical advantage. In this project, a 4-stage different diameter (4 inch, 5 inch, 6 inch and 7 inch) pulley has made for getting different speed. A four-stage pulley has made for motor of diameter 2.5 inch. Variable diameter pulley and motor pulley are shown in the figure 4.5 and figure 4.6 given below.

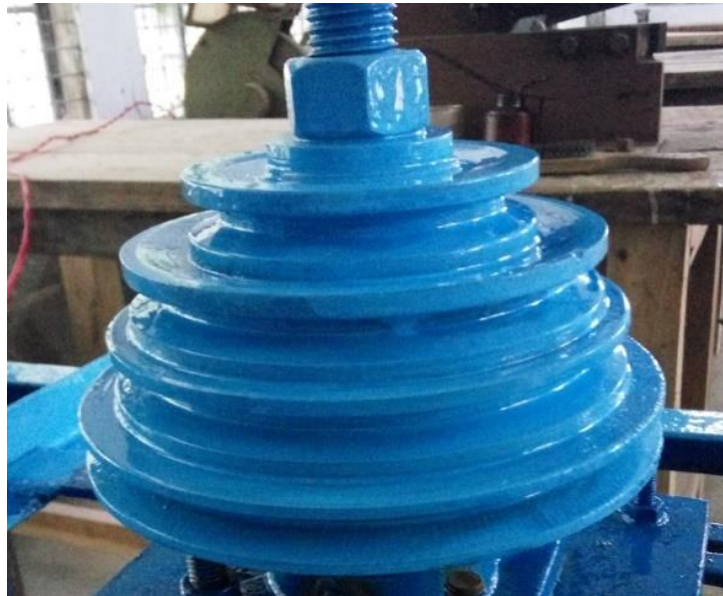


Figure 4.5: Different diameter pulley for shaft.



Figure 4.6: Motor pulley of the erosion tester.

### 4.3.5 Motor

A 220 V single-phase induction motor has used for rotate the shaft as well as sample material. The rated power of the motor is 2 HP and the rated rpm 1450.

### 4.3.6 Fabrication of Control Box.

A control box with dimension 8-inch X 6-inch X 6 inch was made for fixing control switch, protection circuit breaker and motor speed controller. The following equipment has been installed inside the control box. This control box is shown in below figure 4.7 and the main component of this control box are given below.

- a. 4000 W speed controller
- b. Start stop switch
- c. 20 A circuit barker

For speed control, a 4000W variable voltage speed controller was used and for motor over current protection, a 20A circuit barker was used. A push switch was used for quickly start stop the motor.



Figure 4.7: Control box of the slurry erosion tester.

### 4.3.7 Fabrication of Samples

For this experiment, two types of sample were used. One was impeller shape and another flat bar shape, that are shown in below figure 4.8 and figure 4.9.

A solid metal having width 28 mm, thickness of 12 mm and length 190 mm was made for experiment that is shown in figure 4.8. One holes of diameter 16 mm was drilled on the metal strip, one at the center by a universal drilling machine for fitting the spindle with it using a nut.

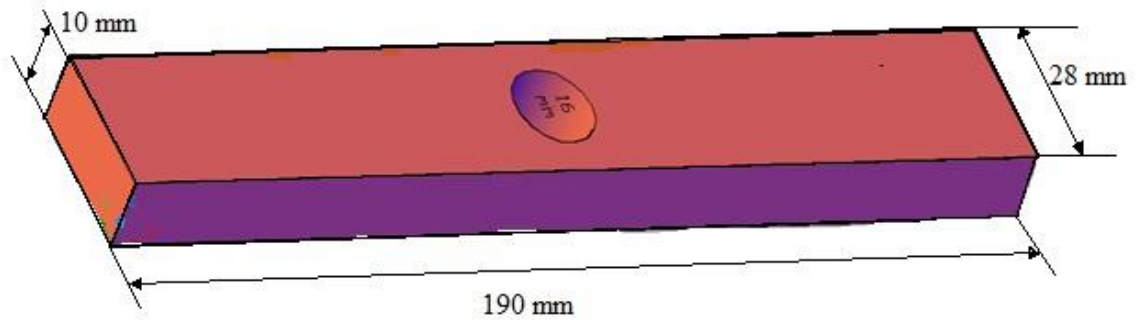


Figure 4.8: Flat bar type sample.

On the other hand, a solid impeller shape sample was prepared for test having impeller width 30 mm, thickness 10 mm and length 190 mm that is shown in figure 4.9. One hole of diameter 16 mm were drilled on the metal strip, one at the center by a universal drilling machine for fitting the spindle with it using a nut.

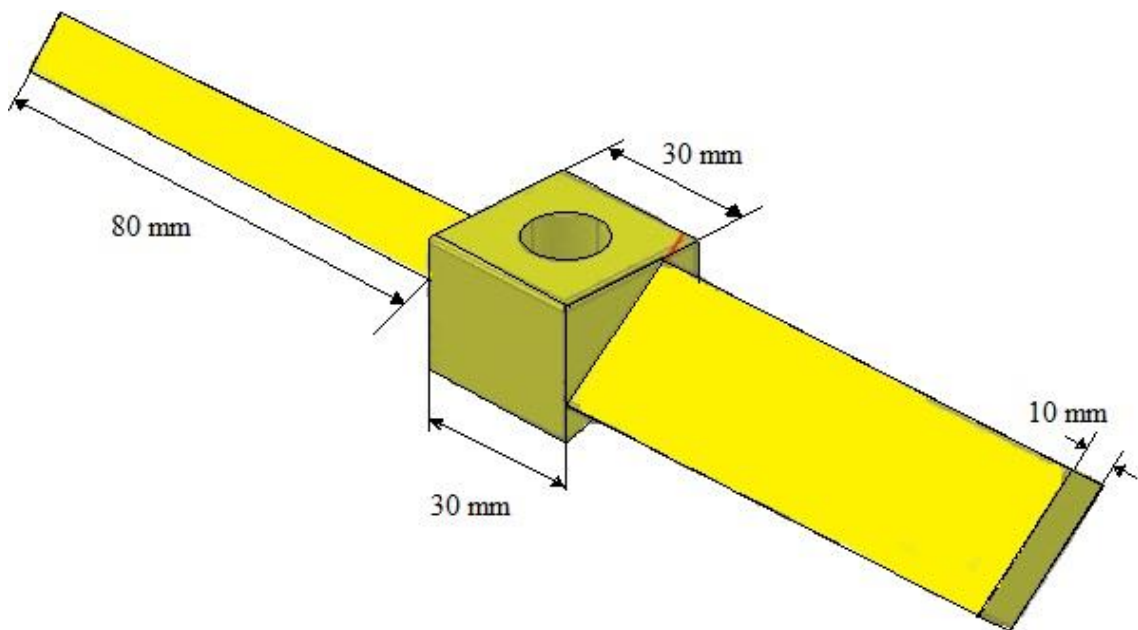


Figure 4.9: Impeller type sample.

#### 4.3.7.1 Aluminum Sample

In below figure 4.10 a flat bar type aluminum sample of having dimension 190 mm x 28 mm x 12mm and in figure 4.11 an impeller type aluminum sample of having dimension 190 mm x 30 mm x 10 mm is shown. This two different geometry aluminum samples were used for the experiment.



Figure 4.10: Flat bar type aluminum sample.



Figure 4.11: Impeller type aluminum sample.

#### 4.3.7.2 Brass Sample

A flat bar type brass sample an impeller type sample are shown in the figure 4.12 and figure 4.13 given below. The dimension of flat bar sample is 190 mm x 28 mm x 12mm and impeller type sample is 190 mm x 30 mm x 10 mm. Both types of sample was made by casting from local market.



Figure 4.12: Flat bar type brass sample.

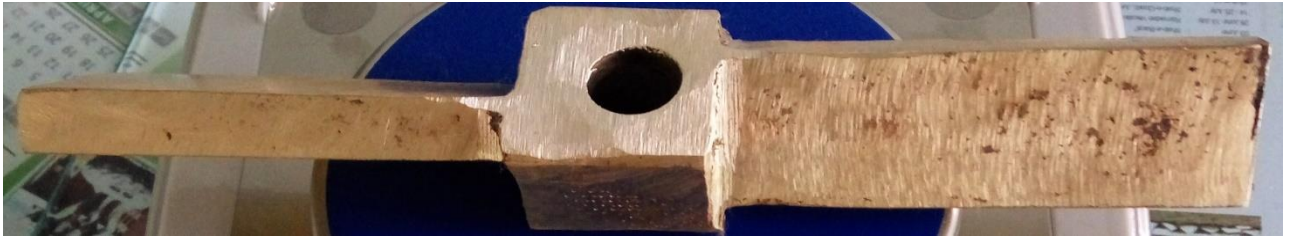


Figure 4.13: Impeller type brass sample.

#### 4.3.7.3 Mild Steel Sample

In below figure 4.14 a flat bar type mild steel sample of having dimension 190 mm x 28 mm x 12mm is shown. This sample was used for the experiment. On the other hand in below figure 4.15 an impeller type mild steel sample of having dimension 190 mm x 30 mm x 10 mm is shown.



Figure 4.14: Flat bar type mild steel sample.



Figure 4.15: Impeller type mild steel sample.

#### 4.3.7.4 Cast-Iron Sample

Cast iron sample are prepared by casing in local market and finally prepared in machine shop. Two different geometry cast iron sample are used for test. In figure 4.16 and figure 4.17 two different geometry sample flat bar and impeller type sample having dimension 190 mm x 28 mm x 12mm and 190 mm x 30 mm x 10 mm are shown.



Figure 4.16: Flat bar type cast iron sample.



Figure 4.17: Impeller type cast iron sample.

#### 4.4 Slurry Erosion Tester Fabrication

The slurry erosion tester is shown in below figure 4.18. This apparatus is a box type arrangement. The major components are structure, motor, slurry pot, shaft, pulley, belt and control box. Main shaft are fixed by pillow type bearing housing. One end of the shaft is fixed with pulley and other end is connected with sample via slurry pot bearing housing. Sample is connected with shaft and fixed by nut bolt. Shaft pulley is connected with motor pulley via a v-belt as a result when the motor starts rotating the shaft holding the samples will also rotate. Slurry pot is fixed with an adjustable height bench and bench height can be adjusted by two screw.



Figure 4.18: Slurry pot tester with different main components.



## 4.5 Working Principle

At first the testing apparatus, slurry pot shaft was cleaned. The slurry was made by silica sand and water by mixing at required ratio. For initial test silica sand and water was mixed at ratio 1:2 (5 kg silica sand and 10 kg water) for the required slurry density  $1105.26 \text{ kg/m}^3$ . By this method, other different density slurry was prepared and shown in below table 4.2.

Table 4.3: slurry properties.

Sl. number	Water(kg)	Sand(kg)	Density( $\text{kg/m}^3$ )	Viscosity(Pa.s )	p <sup>H</sup>
1	10	5	1105.26	$2.24 \times 10^{-04}$	7.4
2	9	6	1129.03	$2.69 \times 10^{-04}$	7.4
3	6	9	1206.89	$4.04 \times 10^{-04}$	7.4

Samples were cleaned by cleaning agent WT-40 and weight by a precision weighing machine. Then the samples were fixed with shaft by fixing bolt. The samples were dipped into the slurry contained in the slurry pot. The motor was then started and the specimens are rotated at the desired speed for a given duration.

After completing the test, samples were removed. Then the samples were firstly clean by clean water and dried. After that, samples were clean by cleaning agent WT-40 and dried. Finally weight of samples were taken.

The difference between the initial weight and final weight was the required loss of mass of the samples. By this method, the rate of erosion of different samples (Aluminum, Brass, Cast iron, Mild steel) with respect to various experimental parameters was calculated.

## 4.6 Experimental Parameters:

The various experimental parameters that have to be varied during the test are:

- a) Slurry concentration
- b) Speed of rotation
- c) Distance traversed
- d) Time

## 4.7 Experimental Data of Erosion Measurement

Experimental data with different testing properties of aluminum, brass, mild steel and cast iron are shown in bellow Table 4.4 to Table 4.19.

Table 4.4: Aluminum sample erosion at 45-degree impact angle, different speed and constant density.

Sl. No.	Speed (rpm)	Density (kg/m <sup>3</sup> )	Duration (Hour)	Initial Weight (g)	Final Weight (g)	Erosion (mg)	Average Erosion (mg)
1	530	1105.26	1	215.085	214.392	693	699
2				214.392	213.698	694	
3				213.698	212.986	712	
4	493	1105.26	1	212.986	212.404	582	580
5				212.404	211.82	584	
6				211.820	211.246	574	
7	425	1105.26	1	211.245	210.787	458	462
8				210.787	210.347	440	
9				210.347	209.859	488	

Table 4.5: Aluminum sample erosion at 45-degree impact angle, different speed and various density

Sl. No.	Speed (rpm)	Density (kg/m <sup>3</sup> )	Duration (Hour)	Initial Weight (g)	Final Weight (g)	Erosion (mg)	Average Erosion (mg)
1	530	1105.26	1	209.859	209.149	710	756
2		1129.03		209.149	208.399	750	
3		1206.89		208.369	207.561	808	
4	493	1105.26	1	207.561	206.956	605	627
5		1129.03		206.953	206.328	625	
6		1206.89		206.333	205.683	650	
7	425	1105.26	1	205.695	205.130	565	588
8		1129.03		205.130	204.542	588	
9		1206.89		204.542	203.932	610	

Table 4.6: Aluminum sample erosion at 0-degree impact angle, different speed and constant density.

Sl. No.	Speed (rpm)	Density (kg/m <sup>3</sup> )	Duration (Hour)	Initial Weight (g)	Final Weight (g)	Erosion (mg)	Average Erosion (mg)
1	530	1105.26	1	235.180	234.680	500	502
2				234.680	234.200	480	
3				234.200	233.672	528	
4	493	1105.26	1	233.672	233.244	428	422
5				233.244	232.794	450	
6				232.794	232.405	389	
7	425	1105.26	1	232.405	232.050	355	352
8				232.050	231.690	360	
9				231.690	231.348	342	

Table 4.7: Aluminum sample erosion at 0-degree impact angle, different speed and various density.

Sl. No.	Speed (rpm)	Density (kg/m <sup>3</sup> )	Duration (Hour)	Initial Weight (g)	Final Weight (g)	Erosion (mg)	Average Erosion (mg)
1	530	1105.26	1	231.348	230.836	512	524
2		1129.03		230.836	230.314	522	
3		1206.89		230.314	229.774	540	
4	493	1105.26	1	229.774	229.324	450	464
5		1129.03		229.324	228.862	462	
6		1206.89		228.886	228.406	480	
7	425	1105.26	1	228.406	227.986	420	433
8		1129.03		227.986	227.559	427	
9		1206.89		227.596	227.144	452	

Table 4.8: Brass sample erosion at 45-degree impact angle, different speed and constant density.

Sl. No.	Speed (rpm)	Density (kg/m <sup>3</sup> )	Duration (Hour)	Initial Weight (g)	Final Weight (g)	Erosion (mg)	Average Erosion (mg)
1	530	1105.26	1	695.37	694.297	1073	1037
2				694.297	693.245	1052	
3				693.245	692.259	986	
4	493	1105.26	1	692.259	691.409	850	868
5				691.409	690.497	912	
6				690.497	689.655	842	
7	425	1105.26	1	689.655	688.89	765	734
8				688.89	688.187	703	
9				688.187	687.452	735	

Table 4.9: Brass sample erosion at 45-degree impact angle, different speed and various density.

Sl. No.	Speed (rpm)	Density (kg/m <sup>3</sup> )	Duration (Hour)	Initial Weight (g)	Final Weight (g)	Erosion (mg)	Average Erosion (mg)
1	530	1105.26	1	687.452	686.444	1008	1047
2		1129.03		686.444	685.406	1038	
3		1206.89		685.406	684.310	1096	
4	493	1105.26	1	684.310	683.455	855	906
5		1129.03		683.445	682.565	880	
6		1206.89		682.565	681.583	982	
7	425	1105.26	1	681.583	680.878	705	740
8		1129.03		680.878	680.130	748	
9		1206.89		680.130	679.363	767	

Table 4.10: Brass sample erosion at 0-degree impact angle, different speed and constant density.

Sl. No.	Speed (rpm)	Density (kg/m <sup>3</sup> )	Duration (Hour)	Initial Weight (g)	Final Weight (g)	Erosion (mg)	Average Erosion (mg)
1	530	1105.26	1	785.970	785.360	610	612
2				785.360	784.740	620	
3				784.740	784.132	608	
4	493	1105.26	1	784.132	783.569	563	565
5				783.569	782.983	586	
6				782.983	782.435	548	
7	425	1105.26	1	782.435	781.947	488	484
8				781.947	781.452	495	
9				781.452	780.981	471	

Table 4.11: Brass sample erosion at 0-degree impact angle, different speed and various density.

Sl. No.	Speed (rpm)	Density (kg/m <sup>3</sup> )	Duration (Hour)	Initial Weight (g)	Final Weight (g)	Erosion (mg)	Average Erosion (mg)
1	530	1105.26	1	780.981	780.368	613	642
2		1129.03		780.368	779.726	642	
3		1206.89		779.726	779.053	673	
4	493	1105.26	1	779.053	778.482	571	584
5		1129.03		778.482	777.894	588	
6		1206.89		777.894	777.301	593	
7	425	1105.26	1	777.301	776.833	468	479
8		1129.03		776.833	776.352	481	
9		1206.89		776.352	775.864	488	

Table 4.12: Mild Steel sample erosion at 45-degree impact angle, different speed and constant density.

Sl. No.	Speed (rpm)	Density (kg/m <sup>3</sup> )	Duration (Hour)	Initial Weight (g)	Final Weight (g)	Erosion (mg)	Average Erosion (mg)
1	530	1105.26	1	589.025	588.547	478	473
2				588.547	588.067	480	
3				588.067	587.605	462	
4	493	1105.26	1	587.605	587.193	412	412
5				587.193	586.772	421	
6				586.772	586.37	402	
7	425	1105.26	1	586.37	585.984	386	382
8				585.984	585.616	368	
9				585.616	585.225	391	

Table 4.13: Mild Steel sample erosion at 45-degree impact angle, different speed and various density.

Sl. No.	Speed (rpm)	Density (kg/m <sup>3</sup> )	Duration (Hour)	Initial Weight (g)	Final Weight (g)	Erosion (mg)	Average Erosion (mg)
1	530	1105.26	1	585.225	584.745	480	488
2		1129.03		584.745	584.258	487	
3		1206.89		584.258	583.760	498	
4	493	1105.26	1	583.760	583.358	402	421
5		1129.03		583.358	582.939	419	
6		1206.89		582.939	582.498	441	
7	425	1105.26	1	582.498	582.126	372	389
8		1129.03		582.126	581.735	391	
9		1206.89		581.735	581.330	405	

Table 4.14: Mild Steel sample erosion at 0-degree impact angle, different speed and constant density.

Sl. No.	Speed (rpm)	Density (kg/m <sup>3</sup> )	Duration (Hour)	Initial Weight (g)	Final Weight (g)	Erosion (mg)	Average Erosion (mg)
1	530	1105.26	1	633.630	633.464	166	165
2				633.464	633.293	171	
3				633.293	633.135	158	
4	493	1105.26	1	633.135	632.994	141	135
5				632.994	632.856	138	
6				632.856	632.729	127	
7	425	1105.26	1	632.729	632.617	112	119
8				632.617	632.498	119	
9				632.498	632.373	125	

Table 4.15: Mild Steel sample erosion at 0-degree impact angle, different speed and various density.

Sl. No.	Speed (rpm)	Density (kg/m <sup>3</sup> )	Duration (Hour)	Initial Weight (g)	Final Weight (g)	Erosion (mg)	Average Erosion (mg)
1	530	1105.26	1	632.373	632.213	160	168
2		1129.03		632.213	632.044	169	
3		1206.89		632.044	631.869	175	
4	493	1105.26	1	631.870	631.719	151	158
5		1129.03		631.719	631.561	158	
6		1206.89		631.557	631.391	166	
7	425	1105.26	1	631.391	631.261	130	136
8		1129.03		631.261	631.126	135	
9		1206.89		631.122	630.980	142	

Table 4.16: Cast Iron sample erosion at 45-degree impact angle, different speed and constant density.

Sl. No.	Speed (rpm)	Density (kg/m <sup>3</sup> )	Duration (Hour)	Initial Weight (g)	Final Weight (g)	Erosion (mg)	Average Erosion (mg)
1	530	1105.26	1	600.63	600.239	391	385
2				600.239	599.853	386	
3				599.853	599.473	380	
4	493	1105.26	1	599.473	599.184	289	309
5				599.184	598.874	310	
6				598.874	598.546	328	
7	425	1105.26	1	598.546	598.235	311	216
8				598.235	598.016	219	
9				598.016	597.897	119	

Table 4.17: Cast Iron sample erosion at 45-degree impact angle, different speed and various density.

Sl. No.	Speed (rpm)	Density (kg/m <sup>3</sup> )	Duration (Hour)	Initial Weight (g)	Final Weight (g)	Erosion (mg)	Average Erosion (mg)
1	530	1105.26	1	597.897	597.496	401	410
2		1129.03		597.496	597.086	410	
3		1206.89		597.086	596.665	421	
4	493	1105.26	1	596.665	596.395	270	321
5		1129.03		596.295	595.990	305	
6		1206.89		596.990	596.601	389	
7	425	1105.26	1	596.601	596.383	218	265
8		1129.03		596.383	596.132	251	
9		1206.89		596.132	595.804	328	

Table 4.18: Cast Iron sample erosion at 0-degree impact angle, different speed and constant density

Sl. No.	Speed (rpm)	Density (kg/m <sup>3</sup> )	Duration (Hour)	Initial Weight (g)	Final Weight (g)	Erosion (mg)	Average Erosion (mg)
1	530	1105.26	1	650.365	650.015	350	360
2				650.015	649.653	362	
3				649.653	649.285	368	
4	493	1105.26	1	649.285	648.975	310	289
5				648.975	648.737	238	
6				648.737	648.416	321	
7	425	1105.26	1	648.416	648.298	118	190
8				648.298	648.080	218	
9				648.080	647.845	235	

Table 4.19: Cast Iron sample erosion at 0-degree impact angle, different speed and various density.

Sl. No.	Speed (rpm)	Density (kg/m <sup>3</sup> )	Duration (Hour)	Initial Weight (g)	Final Weight (g)	Erosion (mg)	Average Erosion (mg)
1	530	1105.26	1	647.845	647.455	390	411
2		1129.03		647.455	647.040	415	
3		1206.89		647.040	646.612	428	
4	493	1105.26	1	646.612	646.300	312	340
5		1129.03		646.300	645.952	348	
6		1206.89		645.942	645.580	362	
7	425	1105.26	1	645.580	645.332	248	295
8		1129.03		645.362	645.066	296	
9		1206.89		645.052	644.710	342	

## CHAPTER V

### Results and Discussion

#### 5.1 Erosion Measurement

The self-made slurry erosion tester was used for testing the samples. All sample were cleaned by cleaning agent and recorded initial weight. Samples were fixed with tester and test period. After completing testing period sample was removed from sample holder and cleaned by cleaning agent WT-40. After cleaning final weight has been taken. The difference between two weight is the required erosion. Average erosion with different testing properties of aluminum, brass, mild steel and cast iron are shown in bellow Table 5.1, Table 5.2, Table 5.3 and Table 5.4.

Table 5.1: Impeller type different samples erosion at constant density.

Slurry density (kg/m <sup>3</sup> )	Time (hour)	Speed (rpm)	Average Erosion (mg)			
			AL	Brass	MS	CI
1105.26	1	530	699	1037	473	385
		493	580	868	411	309
		425	462	734	381	216

Table 5.2: Flat bar type different samples erosion at constant density.

Slurry density (kg/m <sup>3</sup> )	Time (hour)	Speed (rpm)	Average Erosion (mg)			
			AL	Brass	MS	CI
1105.26	1	530	502	612	165	360
		493	422	565	135	289
		425	352	484	118	190

Table 5.3: Impeller type different samples erosion at constant speed.

Speed (rpm)	Time (hour)	Slurry density (kg/m <sup>3</sup> )	Average Erosion (mg)			
			AL	Brass	MS	CI
530	1	1105.26	710	1008	480	401
		1129.03	750	1038	487	410
		1206.89	808	1096	498	421



Table 5.4: Flat bar type different samples erosion at constant speed.

Speed (rpm)	Time (hour)	Slurry density (kg/m <sup>3</sup> )	Average Erosion (mg)			
			AL	Brass	MS	CI
530	1	1105.26	512	613	160	390
		1129.03	522	642	169	415
		1206.89	540	673	175	428

### 5.1.1 Erosion of Aluminum Sample

The developed testing apparatus was successfully measured erosion of aluminum sample with two different geometries. The value of erosion in a certain time and different testing condition such as density of slurry, attack angle, speed and time was determined and shown in above Table 5.1, Table 5.2, Table 5.3 and Table 5.4. All experiments was performed in absence of any kind of corrosive medium and P<sup>H</sup> value of slurry was 7.4. The effect of wear is more at leading edge than at trailing edge of every samples.

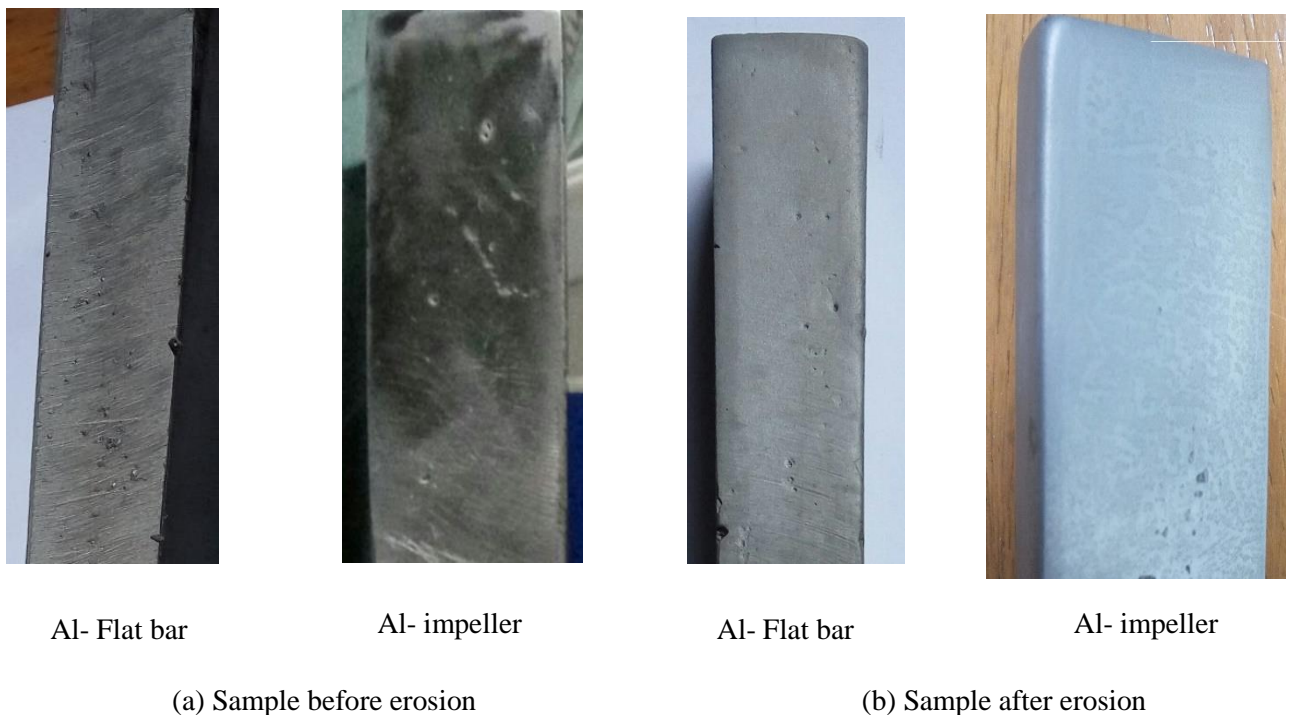
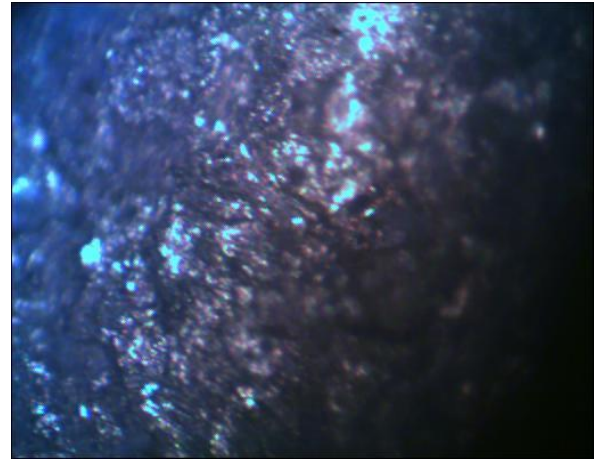
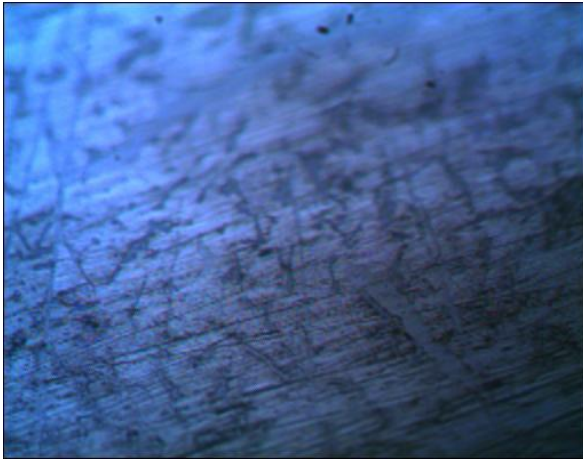


Figure 5.1: Erosion of aluminum sample.

In the above figure, 5.1 (a) two initial Aluminum sample of different geometry are shown and in the figure 5.1 (b) after erosion two Aluminum sample of different geometry are shown. From figure 5.1 (b) it clearly visible that erosion has been occurred and maximum erosion occurred at the leading edge of the sample because of maximum velocity at the top of the sample.

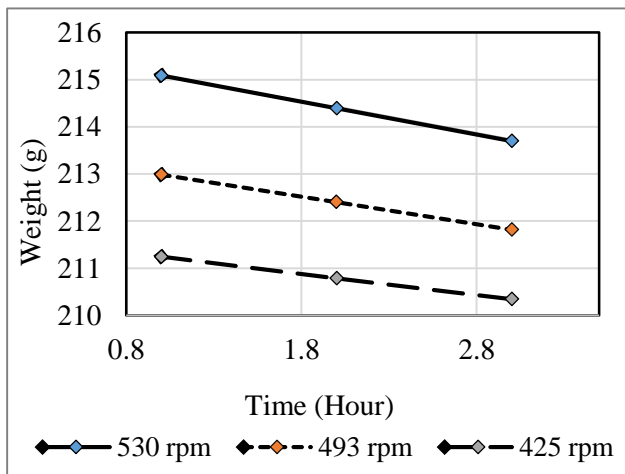


(a) Al sample initial 10X microscopic view.

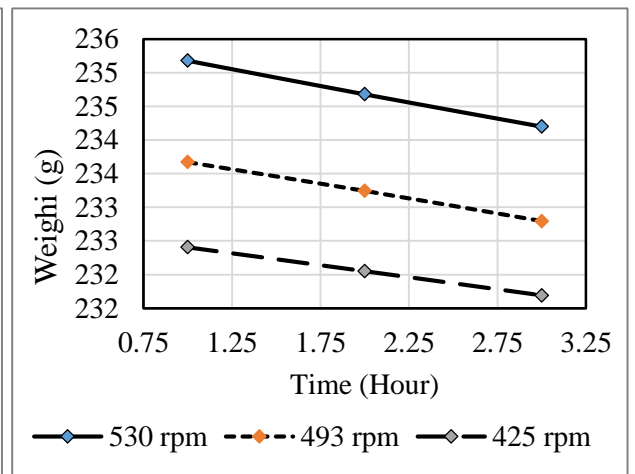
(b) Al sample after erosion 10X microscopic view.

Figure 5.2: Microscopic view of aluminum sample erosion.

In figure 5.2 (a) a microscopic view of aluminum sample before test is shown and from the figure, it is clear that no significant scratch are observed. The sample surface is almost smooth. On the other hand, in figure 5.2 (b) a microscopic view of aluminum sample after test is shown. From the figure, it clear that significant scratch are observed. The sample surface is rough and significant erosion has occurred.



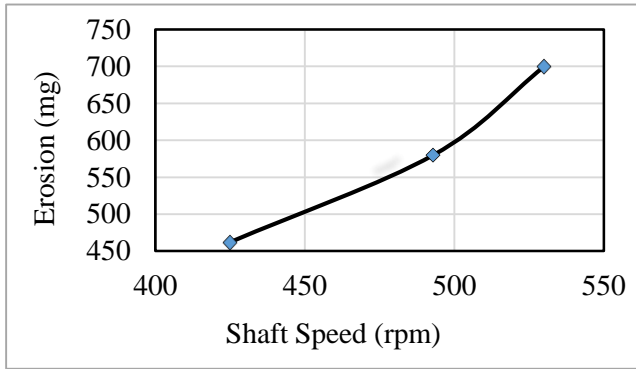
(a) Time vs weight of Al sample at 45° impact angle.



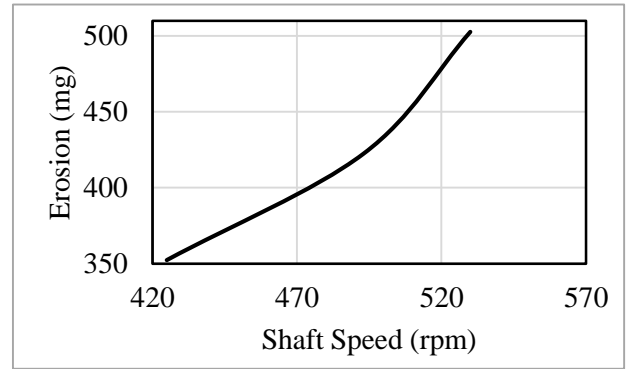
(b) Time vs weight of Al sample at 0° impact angle.

Figure 5.3: Erosion characterizes of Al sample at different speed, impact angle and time.

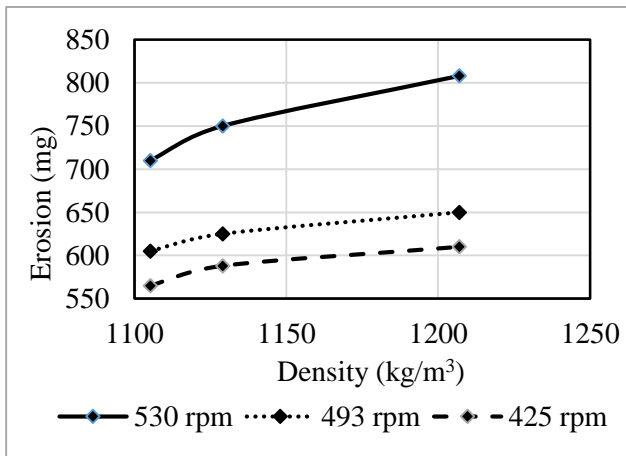
From the above figure 5.3 (a) and figure 5.3 (b), clearly visible that loss of mass increases proportionally due to increase shaft velocity for both type of geometry. Again, from figure 5.3 (a) and figure 5.3 (b), it clearly visible that weight reduction of Al sample at 45° impact angle is higher than the 0° impact angle with respect to time. Therefore, it observe that, if angle of attack is increase, erosion also increase.



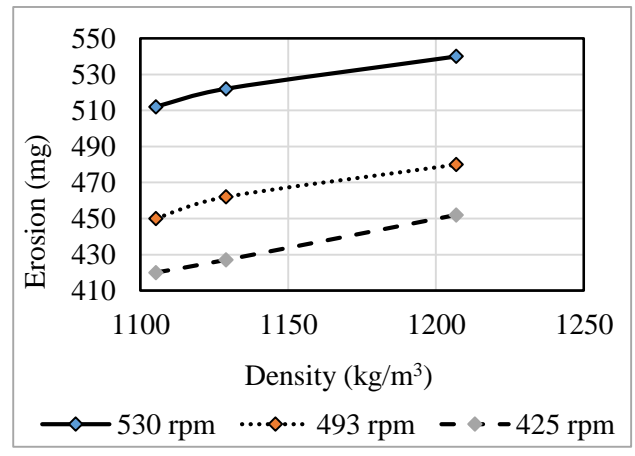
(a) Erosion vs shaft speed characteristic of Al sample at 45° impact angle.



(b) Erosion vs shaft speed characteristic of Al sample at 0° impact angle.



(c) Erosion vs slurry density characteristic of Al sample at 45° impact angle.



(d) Erosion vs density characteristic of Al sample at 0° impact angle.

Figure 5.4: Erosion characteristic of Al sample at different speed, density, impact angle and time.

From the above figure 5.4 (a) and figure 5.4 (b), clearly observe that, erosion almost linearly increase due to increase shaft velocity for both type of geometry. From the above figure 5.4 (c) and figure 5.4 (d) it clear that, erosion proportionally increase due to increase slurry density for both type of geometry.

### 5.1.2 Erosion of Brass Sample

The developed testing apparatus has been successfully measured erosion of brass sample with two different geometries. The value of erosion in a certain time and different testing condition such as density of slurry, attack angle, speed and time was determined which is shown in Table 5.1, Table 5.2, Table 5.3 and Table 5.4. All experiments has performed in absence of any kind of corrosive medium and P<sup>H</sup> value of slurry was 7.4. The effect of wear is more at leading edge than at trailing edge of every samples.



Br- Flat bar



Br- impeller



Br- Flat bar



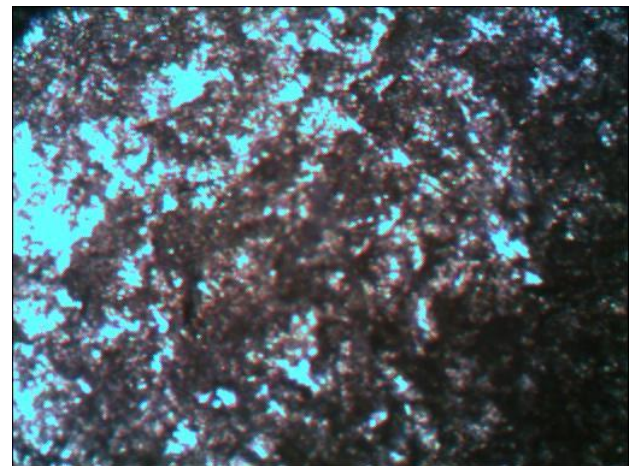
Br- impeller

(a) Sample before erosion.

(b) Sample after erosion.



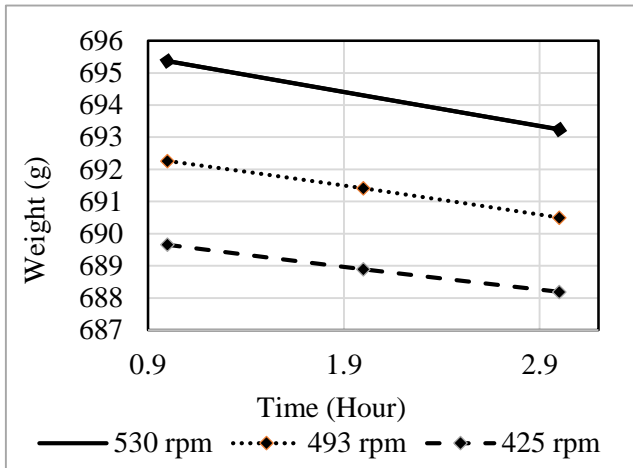
(c) Br sample initial 10X microscopic view.



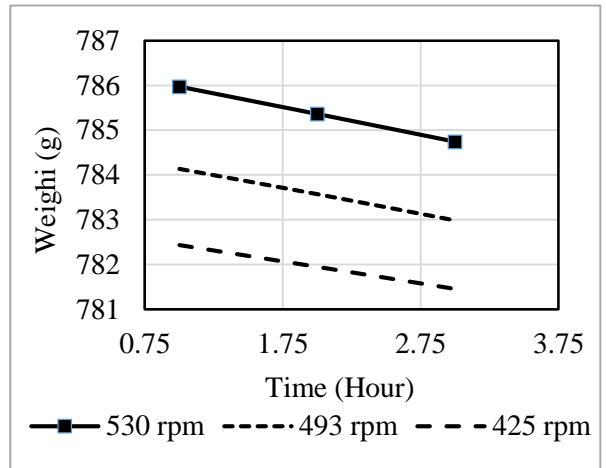
(d) Br sample after erosion 10X microscopic view.

Figure 5.5: Erosion of brass sample.

In the above figure, 5.5 (a) two initial brass sample of different geometry are shown and in the figure 5.5 (b) after erosion brass sample of different geometry are shown. From figure 5.5 (b) it is clearly visible that erosion has been occurred and maximum erosion occurred at the top of the sample because of maximum velocity at the top of the sample. In figure 5.5 (c) a microscopic view of brass sample before test is shown and from the figure, it is clear that no significant scratch are observed. The sample surface is almost smooth. On the other hand, in figure 5.5 (d) a microscopic view of brass sample after test is shown. From the figure, it seen that significant scratch are observed. The sample surface is rough and significant erosion has occurred.



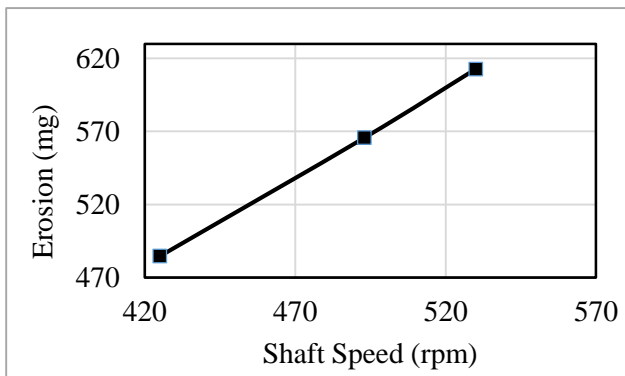
(a) Weight vs time of Br sample at 45° impact angle and constant density.



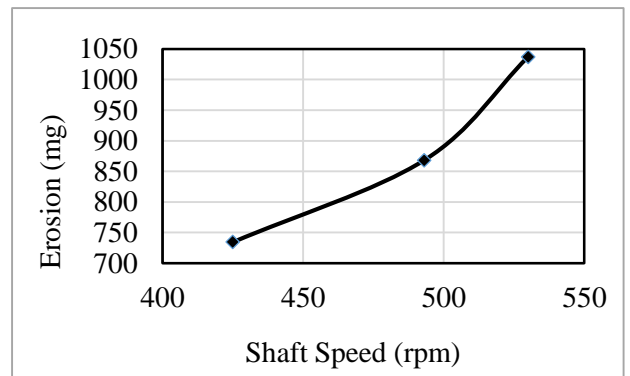
(b) Weight vs time at constant density of Br sample at 0° impact angle.

Figure 5.6: Erosion characterizes of Br sample at different speed, impact angle and time.

From the above figure 5.6 (a) and 5.6 (b), it clearly visible that loss of mass has been proportionally increase due to increase shaft velocity for both type of geometry. From the above figure 5.6 (a) and 5.6 (b) it observe that weight reduction rate of 45° impact angle is higher than the 0° impact angle sample.



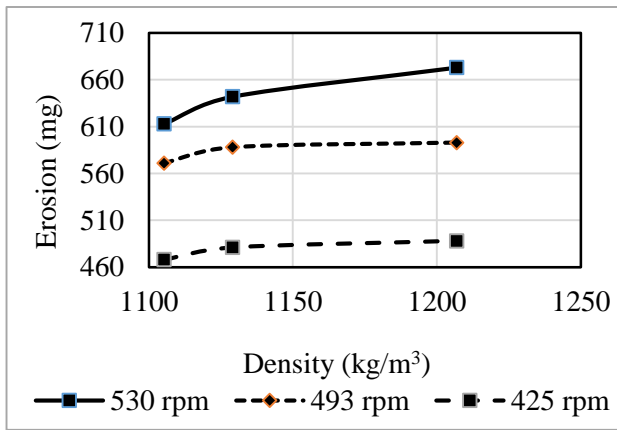
(e) Erosion vs shaft speed of Br sample at 0° impact angle and constant density.



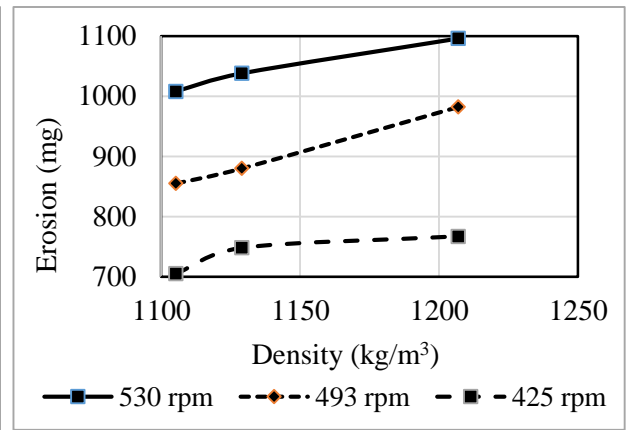
(b) Erosion vs shaft speed of Br sample at 45° impact angle and constant density.

Figure 5.7: Erosion characterizes of Br sample at different speed and impact angle.

From the above figure 5.7 (a) it observe that erosion that erosion linearly increase. From the above figure 5.7 (b) it observe that erosion almost linearly increase due to increase shaft speed.



(a) Erosion vs slurry density of Br sample at 0° impact angle.



(b) Erosion vs slurry density of Br sample at 45° impact angle.

Figure 5.8: Erosion characterizes of Br sample at different speed, density, impact angle and time.

From the above figure 5.8 (a) and 5.4 (b), clearly observe that erosion is proportionally increase due to increase slurry density for both type of geometry.

### 5.1.3 Erosion of Cast Iron

The developed testing apparatus has been successfully measured erosion of cast iron sample with two different geometries. The value of erosion in a certain time and different testing condition such as density of slurry, attack angle, speed and time was determined which is shown in above Table 5.1, Table 5.2, Table 5.3 and Table 5.4. All experiments has performed in absence of any kind of corrosive medium and P<sup>H</sup> value of slurry was 7.4. The effect of wear is more at leading edge than at trailing edge of every samples.

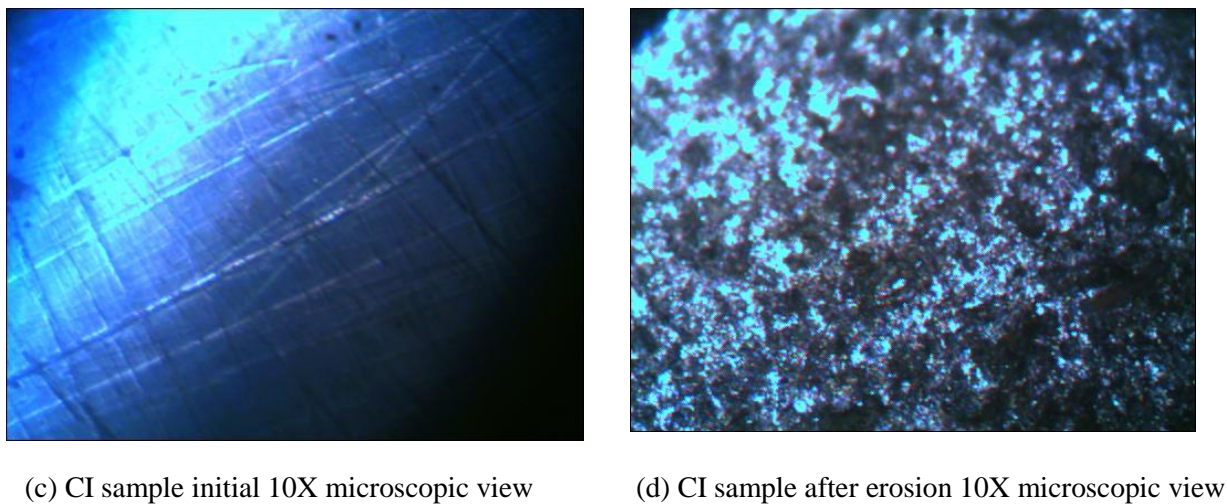
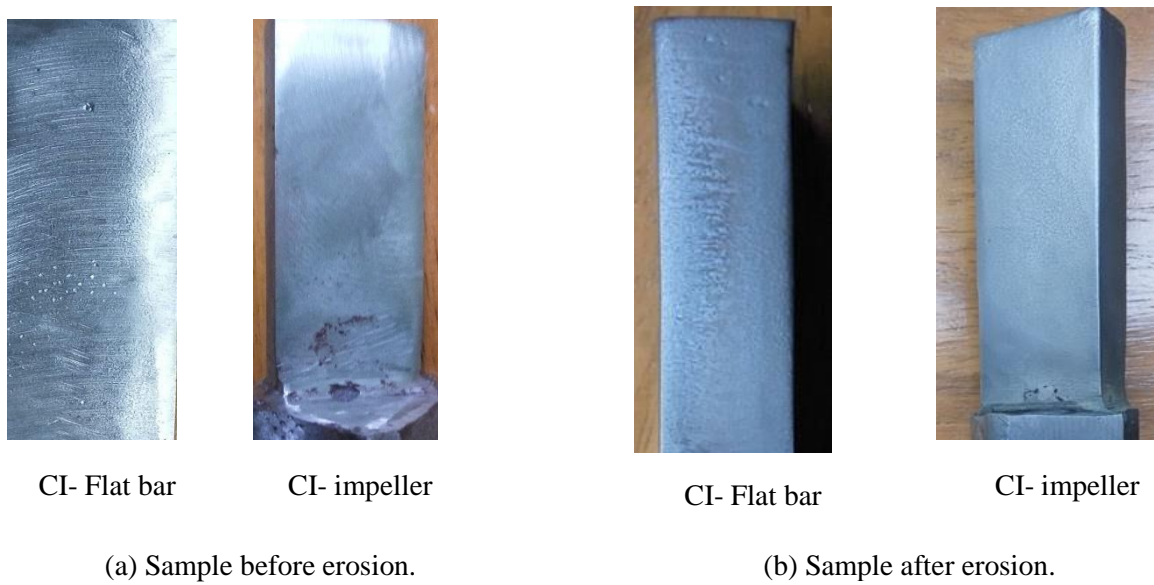
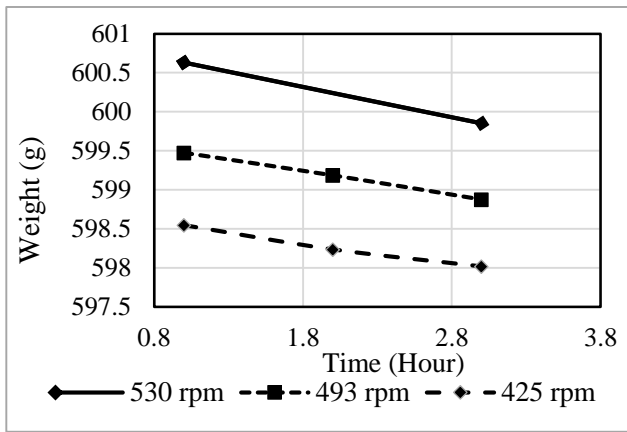


Figure 5.9: Erosion of Cast irons ample.

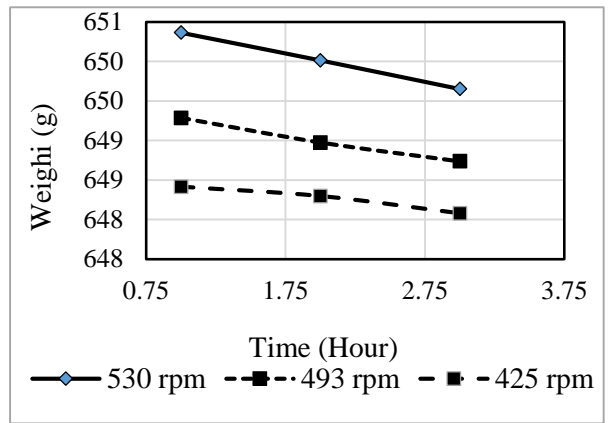
In the above figure, 5.9 (a) two initial cast iron sample of different geometry are shown and in the figure 5.9 (b) after erosion cast iron sample of different geometry are shown. From figure 5.9 (b) it clearly visible that erosion was occurred and maximum erosion occurred at the leading edge of the sample because of maximum velocity at the leading edge of the sample.

In figure 5.9 (c) a microscopic view of brass sample before test is shown and from the figure, it clear that no significant scratch are observed. The sample surface is almost smooth.

On the other hand, in figure 5.9 (d) a microscopic view of brass sample after test is shown. From the figure, it clear that significant scratch are occurred. The sample surface is rough and significant erosion was take place.



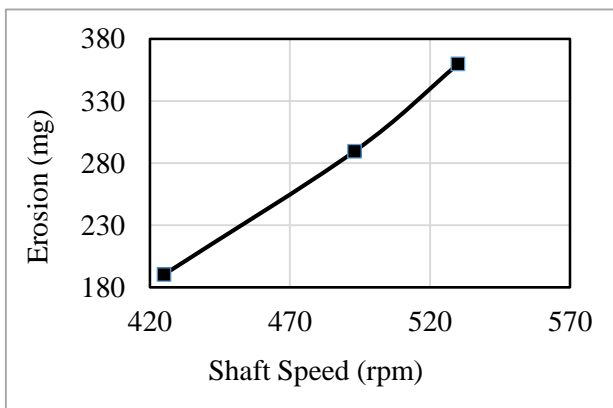
(a) Weight varies with time of CI sample at 45° impact angle and constant density



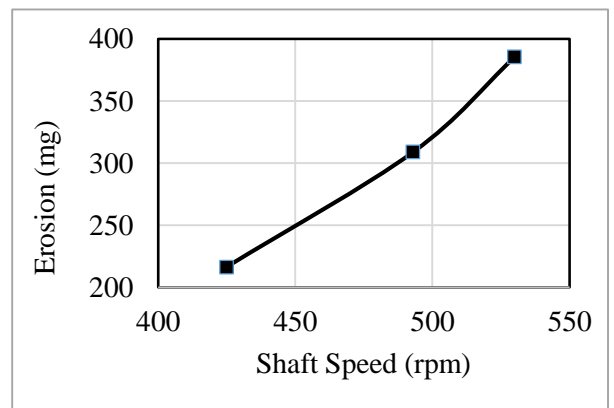
(b) Weight varies with time reduction at constant density of CI sample at 0° impact angle

Figure 5.10: Erosion of CI sample with respect to time at different speed, impact angle, constant density.

From the above figure 5.10 (a) and 5.10 (b), it clearly visible that loss of weight was proportionally increase due to increase shaft speed for both type of geometry. Again, from figure 5.10 (a) and 5.10 (b), it clearly visible that weight reduction of CI sample at 45° impact angle is higher than the 0° impact angle with respect to time. Therefore, if angle of attack is increase, erosion also increase.



(a) Erosion varies with shaft speed of CI sample at 0° impact angle and constant density.

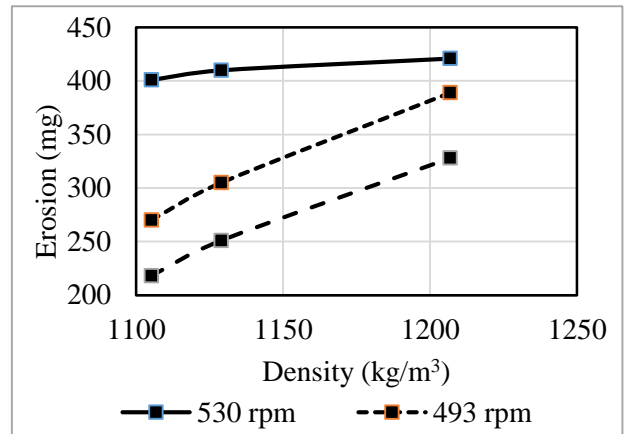
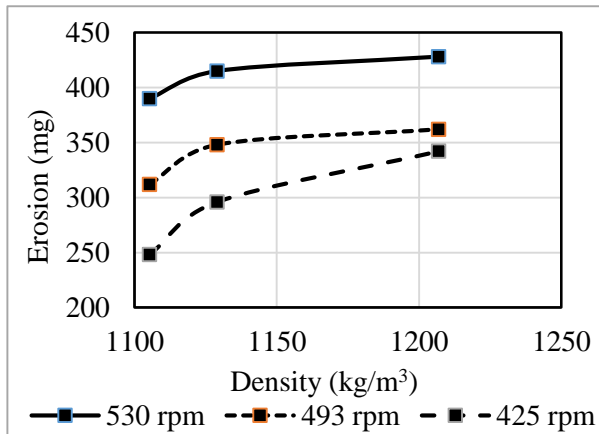


(b) Erosion varies with shaft speed of CI sample at 45° impact angle and constant density.

Figure 5.11: Erosion characterizes of CI sample at different speed, impact angle and constant density.

From the above figure 5.11 (a) and figure 5.11 (b), clearly visible that erosion is almost linearly increase for both type of geometry. From the above figure 5.11 (a) and figure 5.11 (b), it observe that erosion almost linearly increase due to increase shaft speed.





(c) Erosion vs slurry density of CI sample at 0° impact angle.

(b) Erosion vs slurry density of CI sample at 45° impact angle.

Figure 5.12: Erosion characterizes of CI sample at different speed, density, impact angle and time.

From the above figure 5.12 (a) and 5.12 (b), it clear that erosion is increase due to increase slurry density for both type of geometry. From figure 5.12 (a), erosion increases rapidly for a certain slurry density and after that erosion increases linearly with respect to slurry density.

#### 5.1.4 Erosion of Mild Steel

The developed testing apparatus has been successfully measured erosion of brass sample with two different geometries. The value of erosion in a certain time and different testing condition such as density of slurry, attack angle, speed and time was determined which is shown in above Table 5.1, Table 5.2, Table 5.3 and Table 5.4. All experiments has performed in absence of any kind of corrosive medium and P<sup>H</sup> value of slurry was 7.4. The effect of wear is more at leading edge than at trailing edge of every samples



MS- Flat bar



MS- impeller



MS- Flat bar



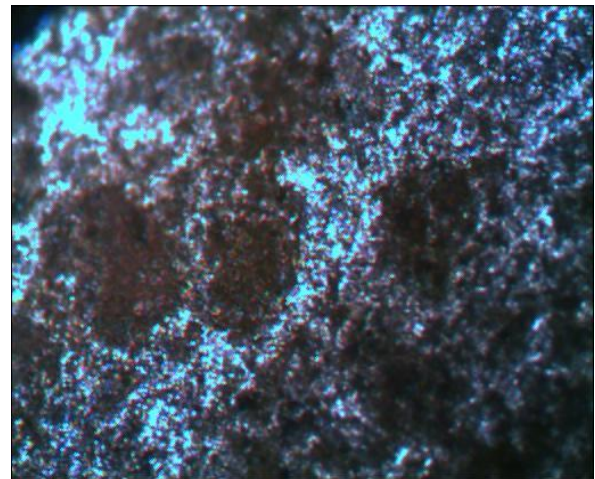
MS- impeller

(a) Sample before erosion.

(b) Sample after erosion.



(c) MS sample initial 10X microscopic view.

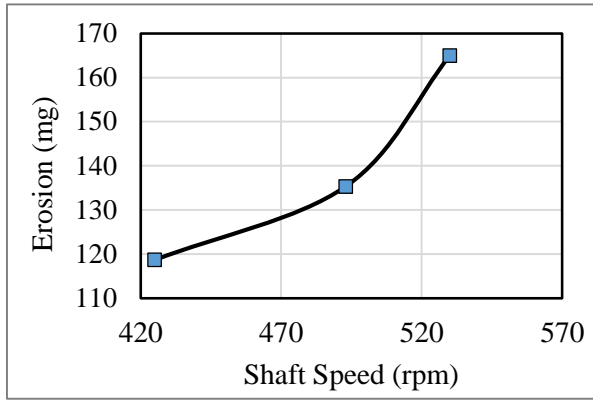


(d) MS sample after erosion 10X microscopic view.

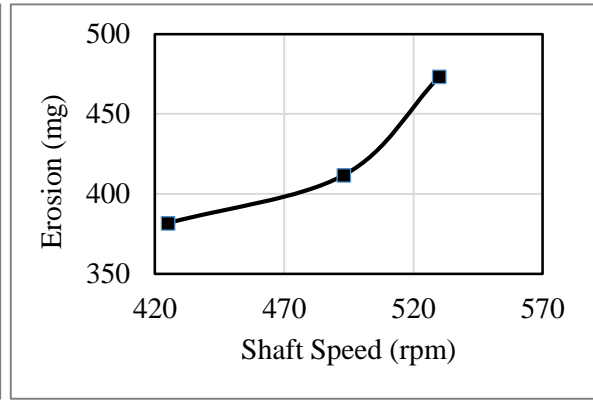
Figure 5.13: Erosion of mild steel sample.

Initial mild steel sample with two different geometry are shown in the above figure 5.13 (a). In figure 5.13 (b) after erosion two mild steel sample with different geometry are shown.

From figure 5.13 (b) it observe that erosion was takes place significantly and maximum erosion occurred at the leading edge of the sample because of maximum velocity at the leading edge of the sample. In figure 5.13 (c) a microscopic view of mild steel sample before test is shown and from the figure, it is clear that no significant scratch are observed and surface is smooth. After test a 10 X microscopic view was taken which is shown in above figure 5.13 (d). From the figure 5.13 (d), it clear that significant scratch are observed. The sample surface is rough and significant erosion was occurred.



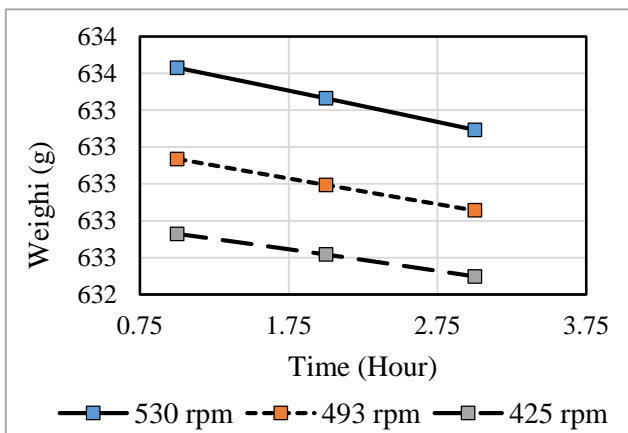
(a) Erosion varies with shaft speed of MS sample at 0° impact angle and constant density



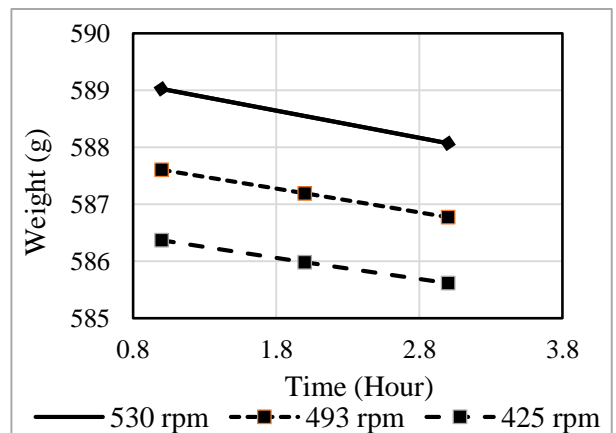
(b) Erosion varies with shaft speed of MS sample at 45° impact angle and constant

Figure 5.14: Erosion characterizes of MS sample at different speed, impact angle and constant density.

From the above figure 5.14 (a) and figure 5.14 (b), clearly visible that erosion is increase for both type of geometry. From the above figure 5.14 (a) and figure 5.14 (b), it observe that erosion almost linearly increase due to increase shaft speed and erosion of 45° -impact angle sample is higher than the 0° -impact angle sample.



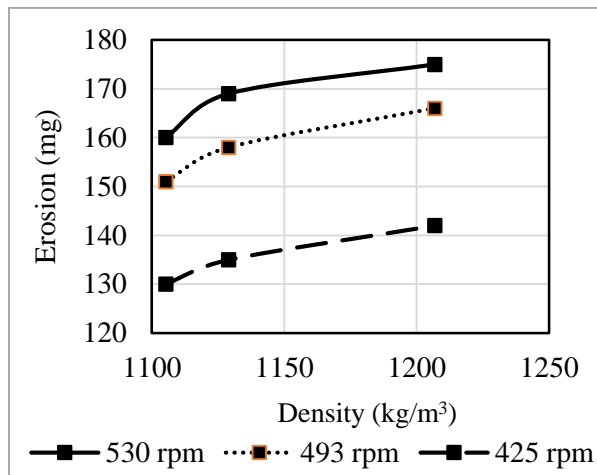
(a) Time vs weight reduction at constant density of MS sample at 0° impact angle.



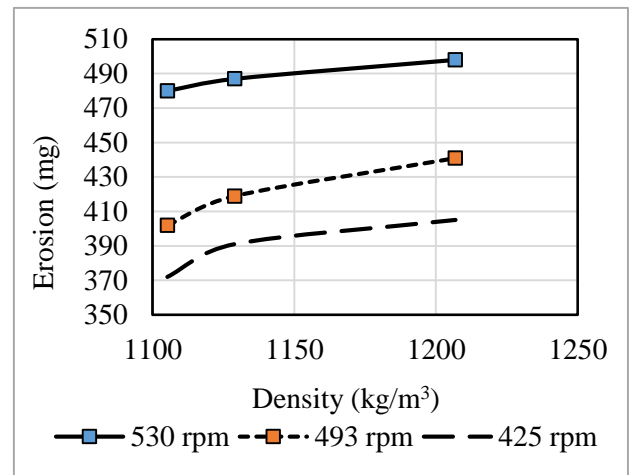
(b) Time vs weight reduction of MS sample at 45° impact angle and constant density.

Figure 5.15: Erosion of MS sample at different speed, impact angle, constant density and time.

From the above figure 5.15 (a) and 5.15 (b), it clearly visible that loss of weight was proportionally increase due to increase shaft speed for both type of geometry. Again, from figure 5.15 (a) and 5.15 (b), it clearly visible that weight reduction of MS sample at 45° impact angle is higher than the 0° impact angle with respect to time. Therefore, if angle of attack is increase, erosion also increase.



(a) Erosion vs slurry density of MS sample at 0° impact angle.



(b) Erosion vs slurry density of MS sample at 45° impact angle.

Figure 5.16: Erosion of MS sample with respect to slurry density at different speed and impact angle.

From the above figure 5.16 (a) and 5.16 (b), it observe that erosion is increase due to increase slurry density for both type of geometry. From figure 5.16 (a) and figure 5.16 (b) it clear that erosion increases rapidly for a certain slurry density and after that erosion increases linearly with respect to slurry density.

## 5.2 Comparison

In this study, total four types of impeller material with two geometries were used for testing at different operating condition such as impact angle, velocity, density and time. Among of the four material Brass was more erosive in constant density for both type of geometries (Flat bar and Impeller) which was shown in Table 5.1, Table 5.2, Table 5.3 and Table 5.4. All slurry were chemically inert and P<sup>H</sup> value of used slurry was 7.4.

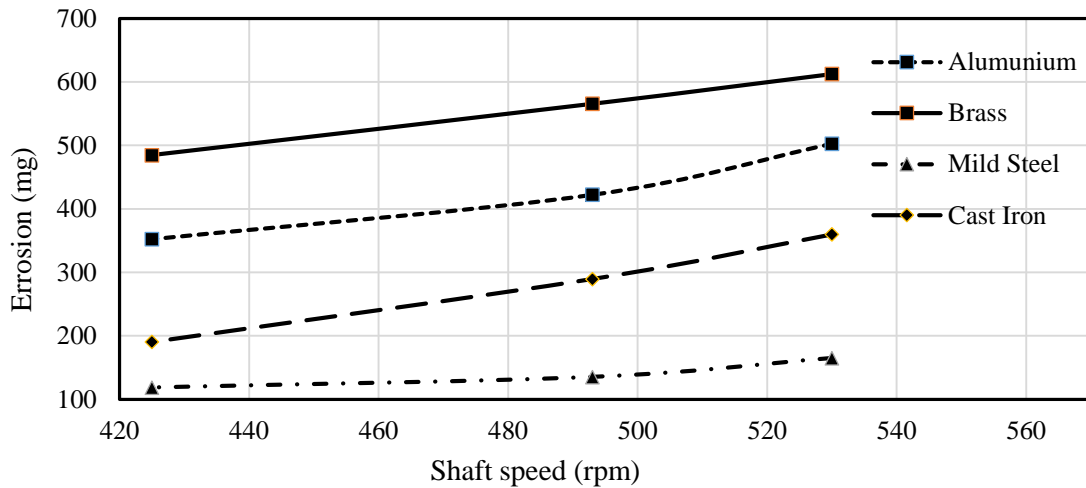


Figure 5.17: Erosion varies with shaft speed at 0-degree impact angle and constant density.

In figure 5.17 relation between erosion and shaft speed for all samples at 0-degree impact angle and constant density are shown. From figure 5.17, it observed that, erosion of brass sample is higher than the others sample. Minimum erosion occurs for mild steel sample. Brass sample erosion is linear with respect to shaft speed and mild steel sample is almost linear. From figure 5.17, it also observed that, erosion of all materials are increase due to increase the shaft speed.

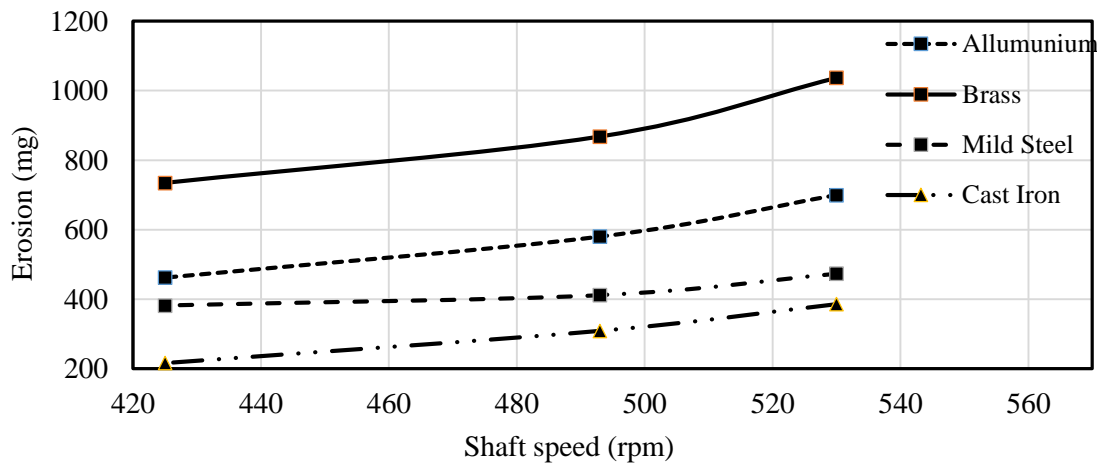


Figure 5.18: Erosion varies with shaft speed at 45-degree impact angle and constant density.

Relation between erosion and shaft speed for all samples at 45-degree impact angle and constant density are shown in figure 5.18. From figure 5.18, it clear that, erosion of brass sample is higher than the others sample. Minimum erosion occurs for cast iron sample. Brass sample erosion is linear with respect to shaft speed and cast iron sample is almost linear. From figure 5.18, it is also observed that, erosion of all materials are increase due to increase of shaft speed.

From figure 5.17 and figure 5.18, it clear that cast iron is best impeller material for 45-degree impact angle and mild steel is best impeller material for 0-degree impact angle.

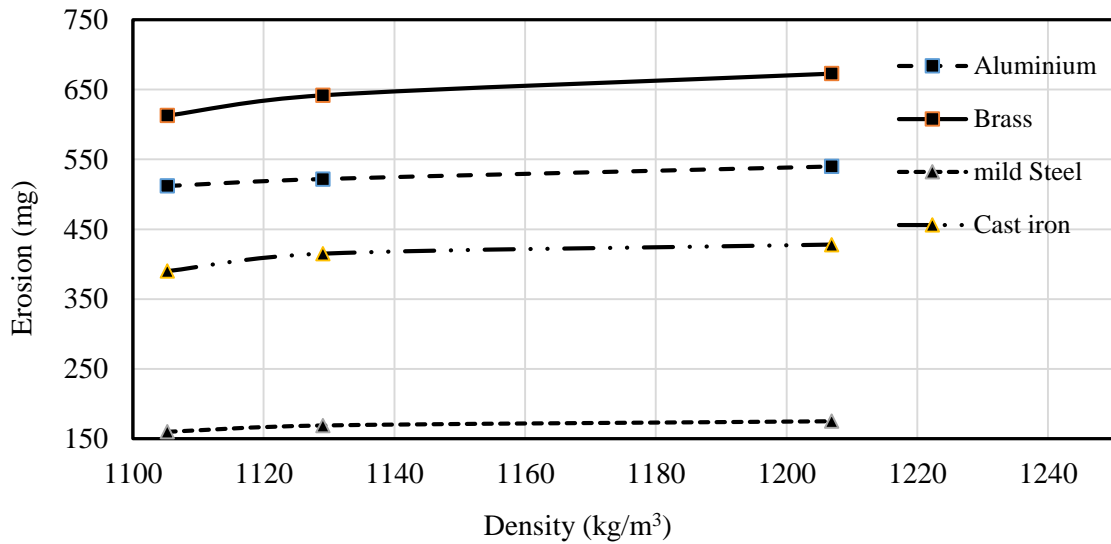


Figure 5.19: Erosion varies with slurry density at 0-degree impact angle and constant speed.

From figure 5.19 seen that erosion of all materials increase almost linearly due to increase of slurry density. From figure 5.19, it observe that, erosion of brass is higher than other materials and minimum erosion occurs for mild steel.

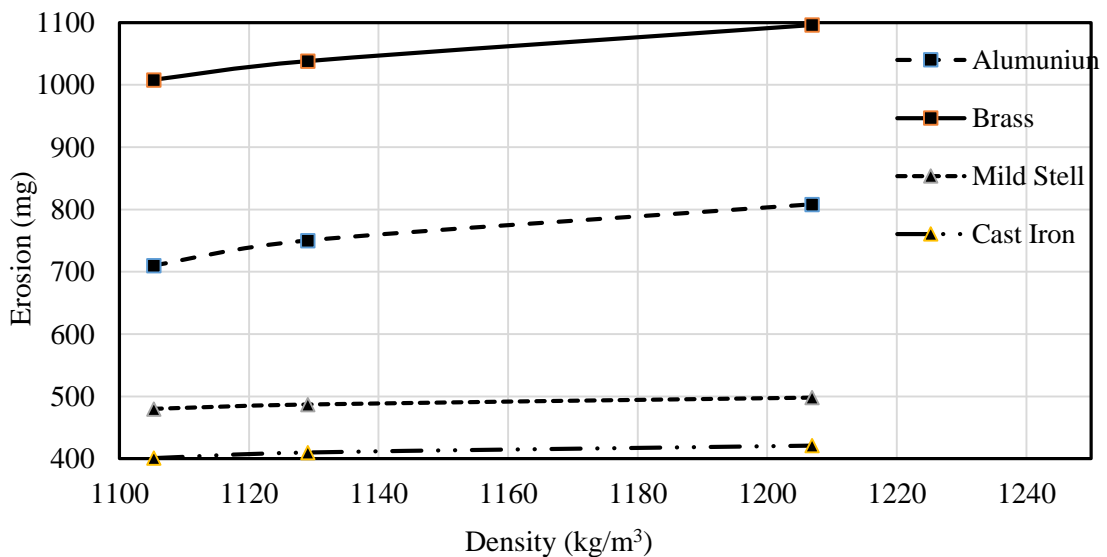


Figure 5.20: Erosion varies with slurry density at 45-degree impact angle and constant speed.

In figure 5.20 shows the relation between erosion and slurry density for all materials at 45-degree impact angle and constant speed. From figure 5.20, it seen that, erosion of brass sample is higher than the others materials. Minimum erosion occurs for cast iron material. All materials (Aluminum, Brass, Cast iron, Mild steel) erosion is almost linear with respect to slurry density and erosion of all materials are increase due to increase of slurry density.

From figure 5.19 and figure 5.20, it observe that, cast iron erosion increases with decreases in impact angle. This may be happened due to gray cast iron brittle property and here pre dominant wear phenomenon is scratching mechanism rather than materials deformation.

From figure 5.19 and figure 5.20, it clear that cast iron is best impeller material for 45-degree impact angle and mild steel is best impeller material for 0-degree impact angle.

## CHAPTER VI

### Conclusion

The slurry pot tester has been successfully designed and fabricated. The fabricated slurry pot tester has been used for test mild steel, cast iron, aluminum, brass samples of different geometry, slurry concentration, particle size and time. The result shows that erosion has closely related on velocity, slurry density, impact angle and time. It is found that when the velocity, slurry density, impact angle and time has been increased, wear rate of those materials also increased. The effect of wear is more at leading edge than at trailing edge of every samples. Therefore, selecting the optimized inlet blade angle can play a major role in reducing erosion wear and providing smooth flow of liquid, reducing materials cost, increasing lifetime and increasing efficiency of the impeller materials.

Among of the four impeller materials (Brass, Aluminum, Mild steel and Cast iron), brass is found more erosive at constant and various slurry density, different shaft speed, chemically inert slurry and different impact angle. Most of erosion are occurred at leading edge.

On the other hand, among of the four impeller (Brass, Aluminum, Mild steel and Cast iron), cast iron is less erosive at constant and various density, different speed, chemically inert slurry and 45-degree impact angle. However, for flat bar (0-degree impact angle) type geometry mild steel was less erosive. Most of erosion are occurred at leading edge for all types of geometry and materials.

It can be concluded that the fabricated pot tester can be used to rank the slurry erosive resistance of solids and cast iron is the best impeller material for pumping inert slurry because of low erosive wear.



## FUTURE SCOPE

The use of pump for pumping slurry day by day has increased vastly in our civilized life. Therefore, it is very important to reduce erosion from the related machinery or equipment so that performance, dependability, and operation life of the slurry equipment can be improved. A lot of work can be done in this field.

- This slurry pot tester can be used for testing different types of materials such as metals, minerals, polymers composites, ceramics, coatings and heat-processed samples.
- Various types of slurries, which are mostly used in different industrial application and other application, can be used for finding the wear characteristics of the material in different environment.
- The other affecting design parameters such as inlet blade angle, outlet blade angle, and the number of blades can be changed to find out the effect of erosion rate and developed most effective impeller blade.

## REFERENCES

- 1 Aseem Mishra, 2011, “Study of erosion wear of pump material for handling water ash slurry”, Master of Engineering Report, Department of Mechanical Engineering, Thapar University.
- 2 G.R. Desale, B.K. Gandhi and S.C. Jain, “Improvement in the design of a pot tester to simulate erosion wear due to solid-liquid mixture”, *Wear*, Vol. 259, pp. 196-202.
- 3 M. H. Buszko and A. K. Krella, 2017 “Slurry erosion-design of test devices”, *Advances in materials science*, Vol. 17 pp. 52.
- 4 A.A. Gadhikar, A. Sharma, D.B. Goel and C.P. Sharma, 2011, “Fabrication and Testing of Slurry Pot Erosion Tester”, *Transactions of the Indian Institute of Metals*, Vol. 64, pp. 493.
- 5 Naveen Sani, 2012, “Investigation of erosion wear of slurry pump material”, Master of Engineering Report, Department of Mechanical Engineering, Thapar University.
- 6 W. Zhu and Z. Y. Mao, 1987, “Study of erosion by relatively soft particles”, *Proceedings of International Conference on Wear of Materials*, ASME, pp. 787-796.
- 7 Samarendra Das and Gopal Krishna Nanda, 2007, “Development of an erosion testing machine”, Department of Mechanical Engineering, National Institute of Technology.
- 8 A. Abouel-Kaseme, Y. M. Abd-elrhmane, K. M. Emarae and S. M. Ahmede, 2010, “Design and Performance of Slurry Erosion Tester”, Department of Mechanical Engineering, Egypt.
- 9 Tsai, W., Humphrey, J. A. C., Cornet, I., and Levy, A. V., 1981, “Experimental Measurement of Accelerated Erosion in a Slurry Pot Tester”, *Wear*, pp.289–303.
- 10 Gupta R., Singh S. N. and Sehadri V., 1995, “Prediction of uneven wear in a slurry pipeline on the basis of measurements in a pot tester”, *Wear*, pp. 184, 169–178.
- 11 Clark, H. McI., 2001, “A Re-Examination of the Particle Size in Slurry Erosion”, *Wear*, 248, pp. 147–161.
- 12 Clark, H. McI, 1993, “Test Method and Applications for Slurry Erosion-A Review”, *Tribology*, pp. 113–132.
- 13 Li, Y., Burstein, G. T., and Hutchings, I. M., 1995, “The Influence of Corrosion on the Erosion of Aluminum by Aqueous Silica Slurries,” *Wear*, 186–187, pp.515–522.
- 14 Zu, J. B., Hutchings, I. M., and Burstein, G. T., 1990, “Design of a Slurry Erosion Test Rig”, *Wear*, 140, pp. 331–344.
- 15 Fang, Q., Xu, H., Sidky, P. S., and Hocking, M. G., 1999, “Erosion of Ceramics Materials by a Sand/Water Slurry Jet”, *Wear*, 224, pp. 183–193.

- 16 Tuzson J. J, 1984, “Laboratory Slurry Erosion Tests and Pump Wear Rate Calculations”, *J. Fluids Engineering*, 106 (35).
- 17 Clark H. M., Hawthorne H. M. and Xie Y, 1999, “Wear rates and specific energies of some ceramic, cermet and metallic coatings determined in the Coriolis erosion tester”, *Wear*, 233–235, 319–327.
- 18 Lin F. Y. and Shao H. S, 1991, “Effect of impact velocity on slurry erosion and a new design of a slurry erosion tester”, *Wear*, 143, 231–240.
- 19 Pramod A. Thakur, Hitesh S. Khairnar, Dr. E.R. Deore and S.R. More, 2015, “Development of Slurry Jet Erosion Tester to Simulate the Erosion Wear due to Solid-Liquid Mixture”, SSVPS, S B.S.D. College of Engineering, Dhule, India.
- 20 Gandhi, B. K., Singh, S. N., and Seshadri, V., 1999, “Study of the parametric dependence of erosion wear for the parallel flow of solid-liquid mixtures”, *Tribology International*, Vol. 32, pp. 275-282.
- 21 Amir Mohamed and Elhosiny Ibrahim, 2018, “Power Characteristics of Impellers”, undergraduate Project, Faculty of Mechanical Engineering, Czech Technical University, Prague.

..